UILU-ENG-81-2542

MAXIMUM LOADABILITY OF TRANSMISSION LINES WITH AND WITHOUT VOLTAGE OR VAR CONTROL

T. W. KAY

Power Affiliates Program

Department of Electrical Engineering

University of Illinois at Urbana-Champaign

Urbana, Illinois 61801

PAP-TR-80-4

August 1980

FOREWORD

This technical report is a reprint of the thesis written by Mr. T. W. Kay as partial fulfillment of the requirements for the degree of Master of Science in Electrical Engineering at the University of Illinois. His research was directly supported through the Power Affiliates Program.

P. W. Sauer

Thesis Advisor

August 1980

ACKNOWLEDGMENT

I would like to express my gratitude to Professor P. W. Sauer for his many hours of guidance throughout the preparation of this thesis.

I would also like to thank the members of the Power Affiliates Program for making it financially possible for me to complete my graduate studies.

TABLE OF CONTENTS

LIST OF FIGURES

1. INTRODUCTION

1.1 Motivation

The trend in electrical power transmission in recent years has been in the direction of longer lines at higher voltages. Also, since systems are being loaded at a heavier rate each year, the maximum power transfer of a particular system must be known with more accuracy to insure an acceptable stability margin.

In most cases, the maximum loadability of a system is found using linear programming techniques. In this method, system generation is increased and the power flow in each line is found as a linear function of generation. This power flow is compared with a maximum power flow specified for that specific line. For very short lines, thermal limitations are the constraining factor; for lines of 75-150 miles, voltage drop is the limiting factor. For lines greater than 150 miles, stability will most likely be the limiting factor.

In some linear programs, various graphs are used to find the limit of a particular line. These graphs show maximum power as a function of line length. When finding stability limits, many of these graphs use a maximum angle of 90° across the transmission line with fixed voltage at each end.

This thesis examines the validity of the 90° stability limit for various types of systems. Systems are studied in which the maximum power transfer occurs at an angle much less than 90° and the voltages all remain acceptable. The effect of shunt capacitors, shunt reactors and synchronous condensers on system and single-line stability is examined closely.

This thesis attempts to clarify when certain stability limits can be used with accuracy and when it is necessary to examine the system in more detail.

1.2 Literature Summary

Transmission line limitations have been a subject of interest for many years. In 1941, Edith Clarke and S. B. Crary published an AIEE paper on stability of long distance transmission lines [1]. Clarke and Crary discuss maximum loading of lines 300 miles or less and also of lines greater than 300 miles. It was found that shorter lines could be loaded above 1.0 SIL (Surge Impedance Loading, see Appendix A), but longer lines of 300 miles and above are limited at a comparatively small value of power. The authors suggested that longer lines have intermediate stations with var supply to increase the stability limit. Their paper deals strictly with stability limitations and all voltages are assumed to be 1 per unit. At the time this paper was written, system voltages were considerably smaller than today's and loading limitations were correspondingly smaller.

Perhaps the most well-known work on transmission line limitations was done by H. P. St. Clair in 1953 [2]. St. Clair uses a benchmark value that a transmission line of 300 miles has a loading capability of 1.0 SIL. This benchmark is the result of years of analysis and practical experience [2]. This limitation has a stability margin of 25%. The 300 mile - 1.0 SIL benchmark is then extended to lines of length 50 to 400 miles. If the value is proportionately extended to a 50 mile line using a constant value of length × SIL, the limit of the line would be 6.0 SIL. This level of loading is enormously high for a line of any

length and would require a tremendous amount of vars; therefore, a value of 3.0 SIL is chosen for the 50-mile line on the basis of existing loads on the American Gas and Electric System at that time. A more conservative curve is offered for systems where var capacity may be very limited. The curve which St. Clair produced is shown in Figure 1.1. It is important to note that these curves were produced by practical experience with transmission lines and not analytically.

Recently, work by R. D. Dunlop et al. at American Electric Power claims to have reproduced the St. Clair curves by a more analytical derivation [3]. The purpose of this work was to get an accurate extension of the St. Clair curve for EHV and UHV transmission lines. The transmission line studied was in the pi-circuit shown in Figure 1.2. The reactances X_1 and X_2 are equivalent terminal reactances for the sending and receiving ends. These reactances include generators, transformers and transmission lines, and are calculated using a 50 kA fault duty [3]. Thermal limits were not considered in this study since most transmission lines have liberally high thermal limits. The angle across the system (δ_1) is increased, thus increasing power transferred across the line, until either the voltage drop limitation of 5% is reached or the stability limit is reached. The stability limit is found assuming a 90° maximum stability angle and a 30-35% stability margin. This limits the angle δ_1 to about 44°. (see Figure 2.2). This calculation was computerized and the resulting load distance curve corresponded very well with the earlier St. Clair curve. The authors concluded that the loadability curves were a good approximation to line loadability even for EHV and UHV lines.

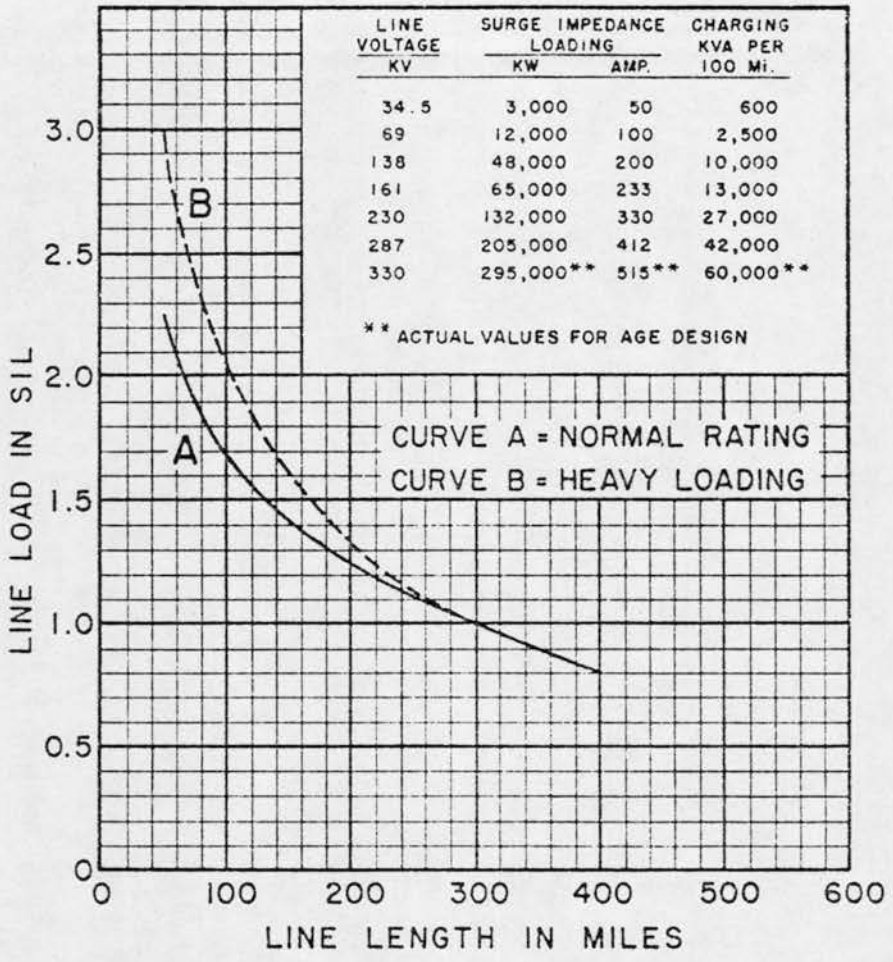

Figure 1.1. St. Clair loadability curve [2].

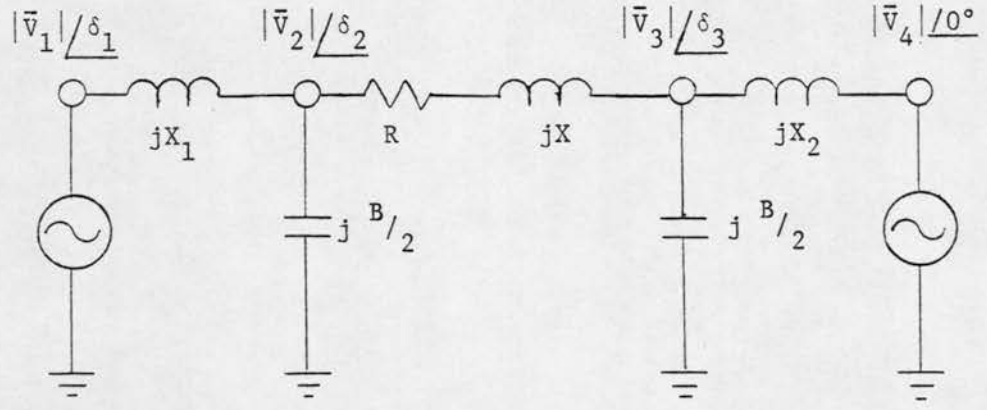

Figure 1.2. Model for analytical derivation of loadability curves.

A different approach was taken to derive loadability curves by Simpson Linke in 1977 [4]. Linke applied the basic L-C model of a transmission line and derived an equation for power transferred across a transmission line. The power transferred is given by Equation (1) [4].

$$P = \frac{m\, E_R^2 \sin \delta_{SR}}{Z_0 \sin \beta x} \tag{1}$$

In Equation 1, m is equal to E_S/E_R, the ratio of sending to receiving end voltage. The angle δ_{SR} is the angular displacement across the line, Z_0 is the characteristic impedance, β is equal to $\sqrt{L/C}$ and x is distance. Since SIL is equal to E_R^2/Z_0, the power transfer in per unit of SIL is given by Equation 2.

$$P_{P.U.SIL} = \frac{m \sin\delta_{SR}}{\sin\beta x} \tag{2}$$

For a given voltage drop across a line of specified distance, the power transfer can be found for any angle δ_{SR} across the line. Depending on the stability margin desired, δ_{SR} can be set at a limiting value and the maximum power transfer calculated. This method assumes that the voltage drop remains constant as δ_{SR} goes from 0 to 90°. In reality, m is a function of δ_{SR} and must be considered in order to find an accurate value of maximum stability angle. When the power-distance curves are plotted for various values of δ_{SR}, the resulting curves are similar to the original St. Clair curves. This method will give accurate results for transmission lines with fixed voltage at each end and unlimited var supply.

A recent report on EHV operating problems notes the importance of voltage control and var allocation [9]. Due to economic reasons, EHV lines are becoming more heavily loaded. Because of this heavy loading,

reactive supply is noted as being increasingly important to maintain system reliability. The importance of optimizing reactive power usage to increase the capacity of EHV lines is stressed.

The above sumaries show that the amount of voltage control and var supply plays an important role in determining the maximum stability limit. This subject is discussed in detail in the following chapter.

2. SINGLE LINE LOADABILITY

2.1 Classical Maximum Power Transfer

In the simplest case, the maximum power transfer of a transmission line connected between two infinite buses is found. This configuration is shown below in Figure 2.1.

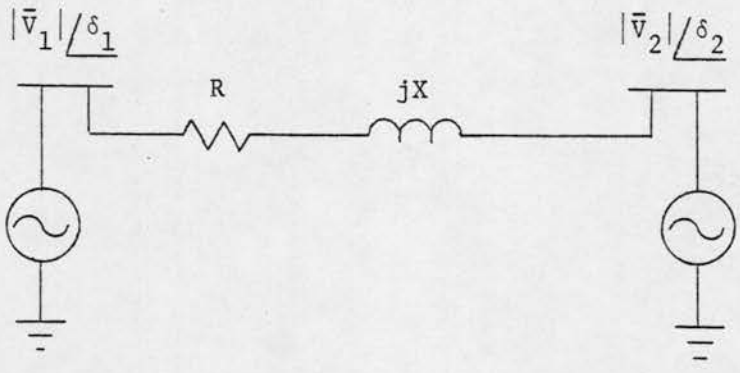

Figure 2.1. Classical model for transmission line.

The power transfer across the line is given by the following equations:

$$P_{12} = \frac{|\bar{V}_1||\bar{V}_2|}{|Z|}\cos(\delta_2 - \delta_1 + \theta_{12}) - \frac{|\bar{V}_2|^2}{|Z|}\cos\theta_{12} \tag{3}$$

$$Q_{12} = \frac{|\bar{V}_1||\bar{V}_2|}{|Z|}\sin(\delta_2 - \delta_1 + \theta_{12}) - \frac{|\bar{V}_2|^2}{|Z|}\sin\theta_{12} \tag{4}$$

where, $|Z| = \sqrt{R^2 + X^2}$

$$\theta_{12} = \tan^{-1}(X/R)$$

These equations give the power transfer from bus 1 to 2 at bus 2. Since the X/R ratio of most lines is around 10, it is a reasonable approximation to consider a lossless line (i.e., R = 0, $\theta_{12} = 90°$). The power flow in this case is given by Equations (5) and (6).

$$P_{12} = - \frac{|\bar{V}_1||\bar{V}_2|}{|Z|} \sin(\delta_2 - \delta_1) \tag{5}$$

$$Q_{12} = \frac{|\bar{V}_1||\bar{V}_2|}{|Z|} \cos(\delta_2 - \delta_1) - \frac{|\bar{V}_2|^2}{|Z|} \tag{6}$$

This power transfer is plotted for fixed $|\bar{V}_1|$ and $|\bar{V}_2|$ as a function of $(\delta_2 - \delta_1)$ in Figure 2.2. This plot shows that

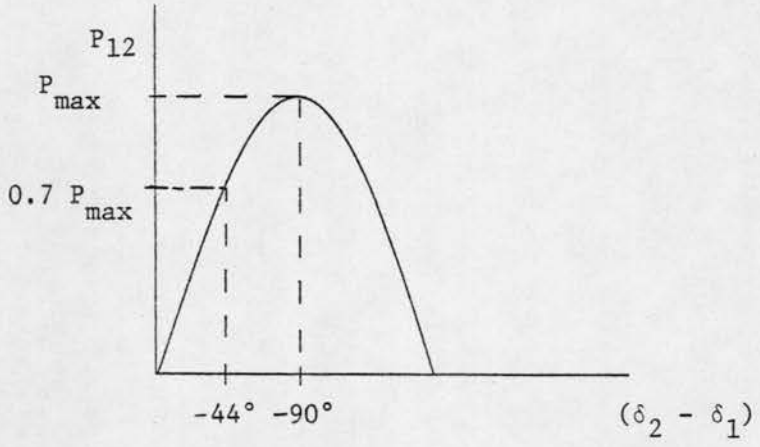

Figure 2.2. Power-angle curve for classical model.

the maximum real power transfer between buses 1 and 2 occurs when the angle $\delta_2 - \delta_1$ is -90°. Equilibrium points with $-90° \leq \delta_2 - \delta_1 \leq -180°$ are unstable. Operation with $\delta_2 - \delta_1 = -44°$ results in a 30% stability margin (70° of maximum power).

It is this classical stability limit of 90° which all of the previously mentioned studies use to define a stability margin. The loadability curves formed by these authors assume that the maximum power transfer is not violated until the angle across the line is 90°, but since this requires perfect voltage

control and thus unlimited reactive power supply, the accuracy of these curves is questionable.

2.2 Loadability Curves

As was mentioned in Chapter 1, the loadability curves of St. Clair were derived mostly from practical experience and were non-analytical. However, the loadability curves of Dunlop et al. of American Electric Power do have an analytical derivation.

The model used for this study was shown in Figure 1.2. The angle δ_1 is claimed to be the angular displacement across the system instead of just across the line itself. The authors justify this by including the two terminal reactances X_1 and X_2 to represent the system to the left and right of the line in the study, respectively. With $|\bar{V}_2|$ and $|\bar{V}_4|$ fixed, and δ_4 equal to 0°, the angle δ_1 is increased until a limit is reached on the magnitude of the voltage $|\bar{V}_3|$ or the angle δ_1 itself. A stability margin of 30-35% is generally desirable in power systems, so a limit on δ_1 should satisfy Equation (7).

$$\frac{\sin \delta_{1max} - \sin \delta_{1L}}{\sin \delta_{1max}} \geq 0.30 \qquad (7)$$

where, δ_{1max} = maximum stability angle

δ_{1L} = limit on δ_1 for stability margin

The authors chose to use the classical stability limit of δ_{1max} equal to 90°; this sets δ_{1L} equal to 44°.

Since the transmission line might be limited by voltage drop instead of stability, a limit for $|\bar{V}_3|$ of 0.95 $|\bar{V}_2|$ is chosen as the voltage constraint. Each time δ_1 is incremented, $|\bar{V}_3|$ is found by Equation 8.

$$\bar{V}_3 = (-\bar{Y}_{32} \, |\bar{V}_2| \, \angle\delta_2 - \bar{Y}_{34} \, |\bar{V}_4| \, \angle 0°)/\bar{Y}_{33} \qquad (8)$$

symbols: $\bar{Y}_{32}$ = admittance of transmission line.

$\bar{Y}_{34}$ = admittance of receiving end terminal.

$\bar{Y}_{33}$ = self-admittance of receiving end of transmission line.

Note: $\bar{Y}_{33} = -\bar{Y}_{32} - \bar{Y}_{34} - \bar{Y}_{30}$.

The angle δ_2 in Equation (8), which is also unknown, can be found as a function of δ_1. This is a rather complicated derivation and is shown in Appendix B.

As the length of the line is increased from 50 to 600 miles, the lines up to 150 miles are limited by the voltage constraint of 0.95 $|\bar{V}_2|$. For lines 200 miles and longer, the limiting factor is δ_{1L}. This agrees with the earlier work of Clarke and St. Clair. However, this author has some doubt of the claim that the angle δ_1 is a good estimation of the system stability.

The model that Dunlop uses is very similar to the classical model except for the terminal reactances. Since the voltages $|\bar{V}_2|$ and $|\bar{V}_4|$ are fixed, and the resistances are small, the maximum power transfer occurs when the angle separating these two buses is 90°. If the terminal reactances are small compared to the line reactance, the angle δ_1 is not much greater than the angle from the sending end of the transmission line to the receiving terminal.

As an example, consider a 345 kV line of 300 miles. A longer line is chosen because it will most likely be limited by stability. From data provided in Dunlops' paper [3], the line reactance is 0.19296 in per unit; the terminal reactances X_1 and X_2 are both 0.00333 per unit. When δ_1 is equal to 90°, the angle at the sending end of the transmission line is 87° while the angle at the receiving end of the line is 3°. When the angle

across the system, as Dunlop defines it, is 90°, the angle across the line is 84°. For most practical purposes, Dunlops' limit is 90° across the line also.

The maximum load this line could transfer using Dunlops' model with a 30% stability margin (δ_{1L} = 44°) is 3.3 per unit. If the classical model is used to find the loadability of the same line, the maximum loadability with a 30% stability margin is 3.45. This is found using Equation (3). There seems to be little difference in the results obtained by using the Dunlop model as opposed to using the classical model. It could then be understood why the loadability curves derived from this model are very similar to the earlier loadability curves which utilized the classical model.

The loadability curves of St. Clair and earlier authors and recently by Dunlop can be accurate if the transmission line is centered in a strong system. In this case, the voltage control at both ends of the line would be good and the model correctly represents the system. Problems arise, however, when transmission lines are in a weak system, or long radial lines serving a distant load are studied. In these cases the amount and type of voltage control at the terminals must be carefully considered when finding the maximum power transfer of the line. This topic is discussed in the next section.

2.3 Voltage Control and Line Loadability

Since all transmission lines have varying degrees of voltage control, it is important to study more than just the classical representation. It is most likely that a line with little or no voltage control might be the limiting factor in the loadability of a system, therefore, it becomes more important to know the stability limit of this line rather than others with good voltage control.

An example of a line which might have limited voltage control is a long radial primary feeder to a distribution substation. It can be assumed that some type of voltage control would exist at the receiving end of the line. A model for this type of line is shown in Figure 2.3.

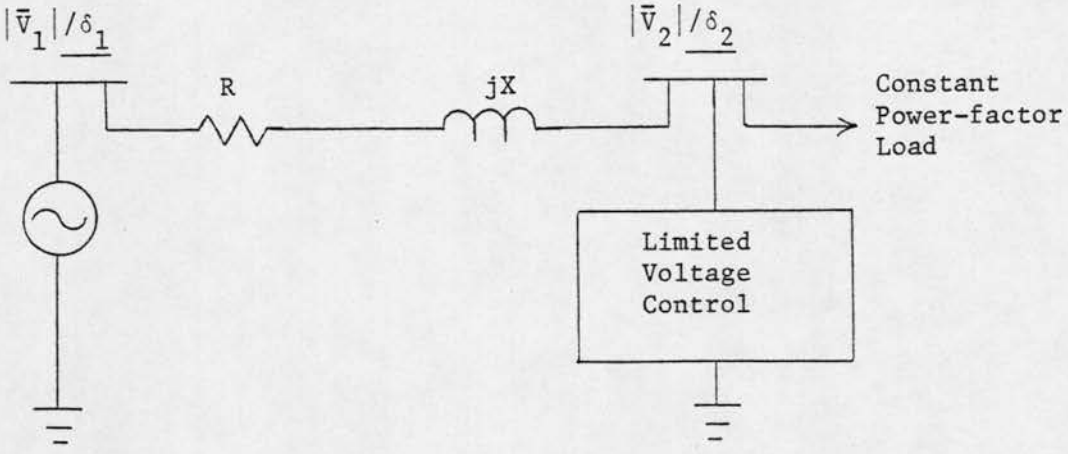

Figure 2.3. Model for long radial line.

Assuming that the power factor of the load is constant, as indicated in the figure, is a fair approximation since the type of load in a particular region is usually homogeneous. (i.e. residential, industrial, etc.) A lossless line is also assumed for reasons discussed in Section 2.1.

This transmission line is simply a generalization of the classical model shown in Figure 2.1. In this case, the voltage at bus 2 is not constant but is dependent on the reactive power supplied at the receiving end. In the following paragraphs, the effectiveness of shunt capacitors and synchronous condensers in increasing the stability limit of the transmission line is discussed.

First, the stability limit of the line with no voltage control is found. The real and reactive power transferred across the line is given by Equations (5) and (6). The equations are the same as those for the classical model except that the voltage $|\bar{V}_2|$ is no longer constant. The maximum power transfer occurs when the derivative of P_{12} with respect to $\delta(\delta = \delta_2 - \delta_1)$ is equal to 0.

$$\frac{dP_{12}}{d\delta} = -\frac{|\bar{V}_1|}{X} \sin\delta \left[\frac{d|\bar{V}_2|}{d\delta}\right] - \frac{|\bar{V}_1||\bar{V}_2|}{X} \cos\delta \tag{9}$$

Since the power factor (PF) and thus reactive power factor (RPF) are constant, Equation (6) can be revised to Equation (10).

$$Q_{12} = \left(\frac{RPF}{PF}\right) P_{12} = \frac{|\bar{V}_1||\bar{V}_2|}{X} \cos\delta - \frac{|\bar{V}_2|^2}{X} \tag{10}$$

Equation (10) and Equation (5) are solved for $|\bar{V}_2|$ and then the derivative of $|\bar{V}_2|$ with respect to δ is taken; the result is shown in Equation (11).

$$\frac{d|\bar{V}_2|}{d\delta} = |\bar{V}_1|\left(\frac{RPF}{PF}\right) \cos\delta - |\bar{V}_1| \sin\delta \tag{11}$$

By using EQuations (11) and (9) the maximum power transfer of the line occurs when the derivative of P_{12} with respect to δ is 0. Solving for δ at this point gives its maximum value for stability. This maximum value of δ is expressed in Equation (12).

$$\tan\delta_{max} - \cot\delta_{max} = 2\left(\frac{RPF}{PF}\right) \tag{12}$$

It should be noted that since δ is equal to $\delta_2 - \delta_1$, it is between 0 and $-90°$ for power to be transferred from bus 1 to bus 2.

Equation (12) indicates that, for a unity power factor load, maximum power transfer occurs at an angle of $\delta_{max} = -45°$. This is the maximum stability angle with no voltage control. A higher angle could be attained with a leading power factor but this is equivalent to voltage control.

An important point must be made here. It is not the magnitude of the voltage $|\bar{V}_2|$ that determines when the maximum stability limit occurs. Rather It is the derivative of $|\bar{V}_2|$ with respect to δ that is the determining factor. This can be seen from Equation (9). Since the limit occurs when the derivative of P_{12} is 0, the value of $d|\bar{V}_2|/d\delta$ at the maximum is given as

$$\frac{d|\bar{V}_2|}{d\delta} = -|\bar{V}_2| \cot \delta \quad . \tag{13}$$

Therefore, it is possible that $|\bar{V}_2|$ can have a very respectable value at the maximum power transfer. Equation (13) also indicates that if $d|\bar{V}_2|/d\delta$ is constantly 0, the maximum stability angle is 90° regardless of the value of $|\bar{V}_2|$. A stability limit of 90° can be attained with $|\bar{V}_2|$ equal to 0.5 per unit, although the power transfer at this point would be only one-half of that with $|\bar{V}_2|$ equal to 1.0 per unit.

The importance of voltage control in power system stability is illustrated in the preceding paragraphs. In power systems today, static capacitors and synchronous condensers are the major types of voltage control used. Shunt reactors are used to limit high voltages at light loading, but since this does not directly affect maximum power transfer they are not discussed here.

Static capacitors are presently the most widely used form of voltage control. Their economical advantage over synchronous condensers and their flexibility in operation make them very popular. However, unless a large amount of capacitance is available with many small switching steps, the amount of voltage control gained is limited. If the capacitor is simply connected to a bus permanently, no improvement is gained in the maximum stability angle; however, there is improvement in the maximum power transfer. For example, suppose a capacitor of susceptance B is connected in shunt at bus 2 of

Figure 2.3. Since Equation (12) is not dependent on shunt or line impedances, δ_{max} is the same as with no capacitor. However, as found in Equation (14) below, for large values of B the magnitude of $|\bar{V}_2|$ at the maximum angle is larger than without the capacitor.

$$|\bar{V}_2| = \frac{|\bar{V}_1|}{x\left(\frac{1}{x} - B\right)} \left[\cos \delta + \left(\frac{RPF}{PF}\right) \sin \delta\right] \tag{14}$$

The derivation of Equations (9)-(14) is shown in Appendix C. The effect of shunt capacitance is to raise the entire power angle curve; however, the maximum occurs at the same angle as with no shunt capacitor. This effect is shown in Figure 2.4

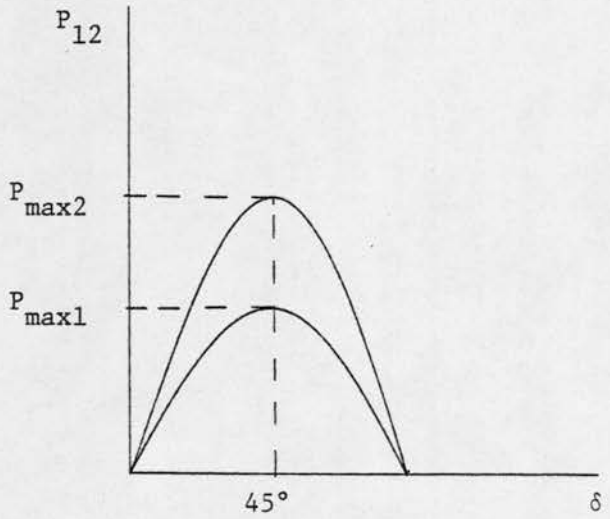

Curve 1 - no shunt capacitor.
Curve 2 - shunt capacitor at bus 2.

Figure 2.4. Effect of shunt capacitor on maximum power transfer.

In many cases, the addition of a shunt capacitor sufficiently increases the stability margin. This can be seen more clearly if the stability margin is defined as in Equation (15).

$$\text{stability margin} = \left[1 - \frac{P_{oper}}{P_{max}}\right] \times 100\% \qquad (15)$$

In Equation (15), P_{oper} is the load that the line carries under normal operating conditions. If P_{max} is increased by 25% by the addition of a shunt capacitor, the stability margin is increased in accordance with Equation (16)

$$SM2 = 0.2 + \frac{SM1}{1.25} \qquad (16)$$

where, SM2 = stability margin after capacitor is added.

SM1 = stability margin before capacitor is added.

As an example of how shunt capacitance could increase the stability margin of a line, consider a lossless line similar to Figure 2.3 of reactance 0.05 per unit serving a unity power factor load. The maximum stability angle for this line is found from Equation (12) to be 45°. If the sending end voltage $|\bar{V}_1|$ is set at 1.0, the voltage $|\bar{V}_2|$ is found from Equation (14) to be 0.707 at 45°. The maximum power transfer is then found from Equation (5) to be 10.0. If under normal operating conditions the line transfers a power of 8.0 per unit, the stability margin of the line is 20% as found from Equation (15). This margin is rather low. As mentioned previously, a stability margin of 30-40% is generally desirable.

To correct this a shunt capacitor of susceptance B = 3.0 is added at bus 2. The maximum stability angle remains at 45°, but the new voltage $|\bar{V}_2|$ is 0.832 per unit. The maximum power transfer is increased to 11.76. The stability margin for normal operating conditions is increased to 32%, an acceptable value.

The above example shows that static capacitors can be helpful in increasing the stability margin of a particular line. In most cases, the capacitors are switched on line in small steps when the voltage gets exceedingly low (below 0.95). The capacitors must also be switched out

under light loading. For instance, if the capacitor of the above example was connected when δ was equal to only 10°, the voltage $|\bar{V}_2|$ would be 1.16 which is unacceptable under any circumstances.

The switching of capacitors also has some positive effect on the maximum stability angle. It can be seen from Equation (9) that the smaller $d|\bar{V}_2|/d\delta$ can be kept, the larger the maximum stability angle will be. The effect of switching capacitors in small steps is to keep $d|\bar{V}_2|/d\delta$ near 0 until either δ is equal to 90° or all of the capacitors are in use.

A transmission line with switched capacitors can be modeled as a line with constant capacitance in between the time two capacitors are switched in. Equation (11) shows that for a given value of δ, $d|\bar{V}_2|/d\delta$ is independent of the magnitude of the susceptance (B). The switching in of a capaciter has the initial effect of increasing the voltage $|\bar{V}_2|$, but any further power demand on the line will force δ to increase and $|\bar{V}_2|$ to decrease at its previous rate. With further increases in power demand, the limit of Equation (13) will eventually be met. At this point, more capacitance is needed for any increase in power transfer. If no more capacitance is available, this point is the maximum power transfer.

By switching capacitors in steps, only the amount of reactive power necessary to supply the increased load is supplied. Once the capacitors are switched in, they are of little help when the voltage begins to drop since the reactive output of the capacitor decreases as the square of the voltage. This is one of the disadvantages of capacitors in a power system. Another form of voltage control that does not have this disadvantage is the use of synchronous condensers.

A synchronous condenser is simply an over-excited synchronous motor with no mechanical load. It responds to a voltage decrease by supplying

more vars to the system, therefore, increasing the voltage. Unlike capacitors which control voltage between set limits, synchronous condesers can control a voltage almost exactly at one level. The synchronous condenser is analogous to a capacitor with infinitely small step sizes, and each step is switched in or out when the voltage deviates from 1.0 per unit.

Although a synchronous condenser uses vars more efficiently than capacitors, they too have a maximum limit which is set by design and operation standards. So the stability limit is dependent upon the maximum amount of reactive power the condenser can supply.

Consider the transmission line of Figure 2.3 with a synchronous condenser attached at bus 2. The synchronous condenser will have some maximum amount of reactive power, Q_{max}, which it can supply the system. Since a synchronous condenser can also absorb vars, it can keep the voltage constant in light loading conditions, a distinct advantage over static capacitors.

The synchronous condenser is set to keep the voltage $|\bar{V}_2|$ at a specified value. The voltage $|\bar{V}_2|$ will remain constant until either the angle across the line is 90° or the maximum capacity of the synchronous condenser, Q_{max}, is reached. If the limit of the synchronous condenser is reached first, the angle across the line at this point is found from the power transfer equations and is expressed in Equation (17).

$$\delta_{max} = \cos^{-1}\left[\frac{|\bar{V}_2|^2\left(\frac{1}{X}+\frac{1}{X_{LC}}\right) - Q_{max}}{\frac{|\bar{V}_1||\bar{V}_2|}{X}}\right] \qquad (17)$$

where, X = line reactance

X_{LC} = line charging reactance

This equation is derived in Appendix D. The value of delta must be between 0 and -90° for power to flow from bus 1 to bus 2.

The value of δ expressed in Equation (15) is also the maximum stability angle of the line in Figure 2.3 with a synchronous condenser connected at bus 2. This can be shown by considering the same line, except with a constant reactive source at bus 2 injecting Q_{const} from zero load to maximum load. The maximum stability angle for this case is also found from the power transfer equations and is expressed in Equation (18).

$$\delta_{max} = \tan^{-1}\left[\frac{4X_s Q_{const} + \sqrt{16X_s^2 Q_{const}^2 + \frac{4|\bar{V}_1|^2}{X^2}\left(4X_s Q_{const} + \frac{|\bar{V}_1|^2}{X^2}\right)}}{\frac{2|\bar{V}_1|^2}{X^2}}\right]^{1/2} \quad (18)$$

This equation is derived in Appendix E. For a given value of Q_{const}, the maximum stability angle given by Equation (18) is less than the maximum angle of Equation (17) with Q_{max} equal to Q_{const}. (Shown below are the two maximum angles for various values of Q.)

Q_{max}, Q_{const}	δ_{max} (Synchronous condenser)	δ_{max} (constant Q)
0*	-48°	-45°
1.0	-66°	-50.5°
2.0	-82°	-57°

*A synchronous condenser with Q_{max} = 0 would be able to absorb vars and keep the voltage constant under light loading. A constant source equal to 0 is equivalent to no shunt compensation.

Note that when the synchronous condenser hits its limit it is already past the stability point of the model with constant Q equal to Q_{max}. After the synchronous condenser hits its var limit, it is equivalent to the constant Q model; and since it is past its stability limit in this case, the line can support no further increases in power transfer.

It should be noted that if series capacitors or shunt reactors are located on the line the limit of Equation (17) is not necessarily greater than that of Equation (18). The reason is that they make the line appear shorter in some ways but not in others, i.e., series capacitors make the line reactance smaller but do not affect the line charging. Therefore, if series capacitors or shunt reactors are included, both limits must be found and the larger one is the maximum stability angle.

Synchronous condensers provide the most accurate form of voltage control in a power system. For a radial line similar to that of Figure 2.3, the maximum stability angle can be found by using Equations (17) and (18). In many cases δ_{max} will be considerably less than 90°. In a study such as that done by Dunlop mentioned earlier in this chapter, the maximum angle across the line should be found by using the correct stability limit and not assuming it to be 90°.

This chapter studied the loadability of a single line. In many power systems, it is possible that a single line may limit the maximum power transfer of the system. If a long line connects two subsystems, the loading limitation of the long line will have a great effect on the maximum loadability of the whole system. This topic is discussed in detail in the next chapter.

3. POWER SYSTEM LOADABILITY

3.1 Introduction

It is of interest to extend the discussion of Chapter 2 to the maximum power transfer of a system. A power system can be limited by two constraints, maximum generation capability and maximum transmission capability. If the limiting constraint is generation, the only way to extend the capacity of the system is to supply more generation. If the limiting constraint is transmission, an improvement in the transmission system must be made to increase the capacity of the system.

The constraint of maximum generation will always be known with exactness since it is just the sum of the maximum output of each generator. However, as was shown in Chapter 2, the transmission capability depends heavily on system parameters; the capability of the same transmission line in two separate systems could be significantly different.

This chapter discusses methods of finding the maximum loadability of a system. An attempt is made to correlate the limits found for a single line in Chapter 2 and the limit of the same line integrated into a system. The purpose is to define a stability limit for a transmission line which could be used in linear programming techniques to find the maximum system capability.

3.2 The Linear Load Flow

A linear load flow gives the change in power flow in a transmission network as a linear function of the change in generation or load on the system. However, a base case solution for the system must be found by an iterative load flow to begin. One example of a linear solution of a system after a change in load schedule is shown in Equation (19).

$$\Delta\bar{S}_{ij} = \sum_{k=1}^{n} \zeta^{*}_{ij,k} \, \Delta\bar{S}_{k} \qquad (19)$$

In this equation, the change in power flow from bus i to bus j is a linear function of the change in load scheduled at each bus. The term $\zeta^{*}_{ij,k}$ is known as a "current" distribution factor and is defined in Equation (20),

$$\zeta_{i,j,k} = \left(\frac{Z_{ik} - Z_{jk}}{z_{ij}} \right) \tag{20}$$

where Z_{ij} are entries of the bus impedance matrix referenced to swing and $\bar{z}_{ij}$ is the primitive impedance between buses i and j, and (.)* denotes conjugation. In Equation (20), $\zeta_{ij,k}$ is the current distribution factor of buses i to j for a change in load schedule at bus k. The derivation of these equations is discussed in detail in reference [7].

Linear techniques similar to those described above were applied by engineers at General Electric to derive a method for finding the maximum capability of a system [6]. In their application, the power transfer of a line is given as a linear function of the generation at each bus. The system generation is maximized using linear programming until either all generation is used or a line is loaded to its maximum. The authors suggested that the loadability curves of Dunlop [3] be used to define the maximum capability of each line. But as discussed in Chapter 2, these limits may not be acceptable for certain lines. Since linear load flows are very advantageous in system capability studies, it is desirable to find an accurate estimate of maximum transmission capability for use in these programs.

In the following sections, an iterative load flow is used to find the maximum capability of a sample system. The limits defined in Chapter 2 for various levels of voltage control are compared with the results obtained from the load flows. An attempt is made to find the limits which prove most accurate for use in a linear load flow.

3.3 Load Flow Studies

One way to find the maximum stability limit of a system is to perform an iterative load flow, increasing the load schedule until the load flow

fails to converge. At this point, the system is at its maximum power transfer. Of course, the maximum could be changed by revising the generation schedule, but this does not affect the purpose of this study and is not done. From the data at the maximum power transfer, the transmission line or lines which are at their limit can be found. These maximum line flows can then be compared with the limits defined in Chapter 2 and those of St. Clair and Dunlop. Hopefully, from these data, criterion for applying certain limits can be found.

A brief flow chart for the program used in this study is shown in Figure 3.1. A Newton-Raphson load flow is used; for more details on this type of load flow see reference [5]. Three types of nodes are used in the load flow; they are the swing, PV and PQ nodes. PV nodes are used to represent generators other than that of the swing bus and also to represent voltage controlled buses. PQ nodes are used to represent load buses.

As mentioned in Chapter 2, loadability curves could give accurate results for systems with good voltage control; however, systems with limited voltage control must be studied in more detail. Both types of systems are studied by the load flow to verify the above claim.

The first system to be studied is shown in Figure 3.3. The long 400-mile line could represent an intertie between two subsystems. Since the 50-mile lines can carry as much as four times the power of the 400-mile lines, it becomes obvious that the loadability of the 400-mile line will be the limiting factor on the system. With generators located at bus 1 and bus 5, the voltage control at each end of the 400-mile line is very strong, which indicates that the loadability curves should accurately predict the maximum power transfer of the line. For convenience, the St. Clair loadability curve for 345 kV is shown in Figure 3.2. The limit for the 400-mile line from the St. Clair curve is 0.8 SIL or 2.56 per unit (SIL = 320 MW).

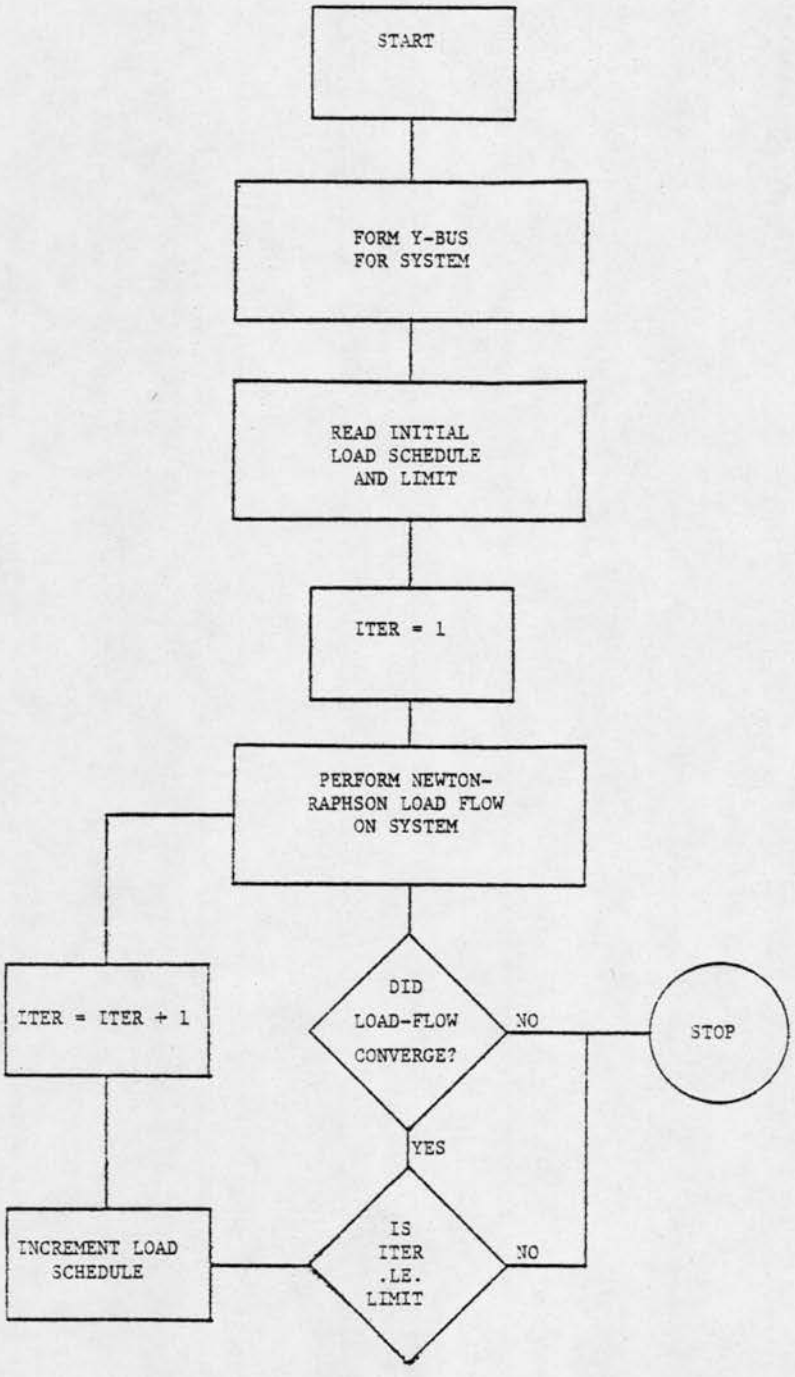

Figure 3.1. Flow chart for load flow study.

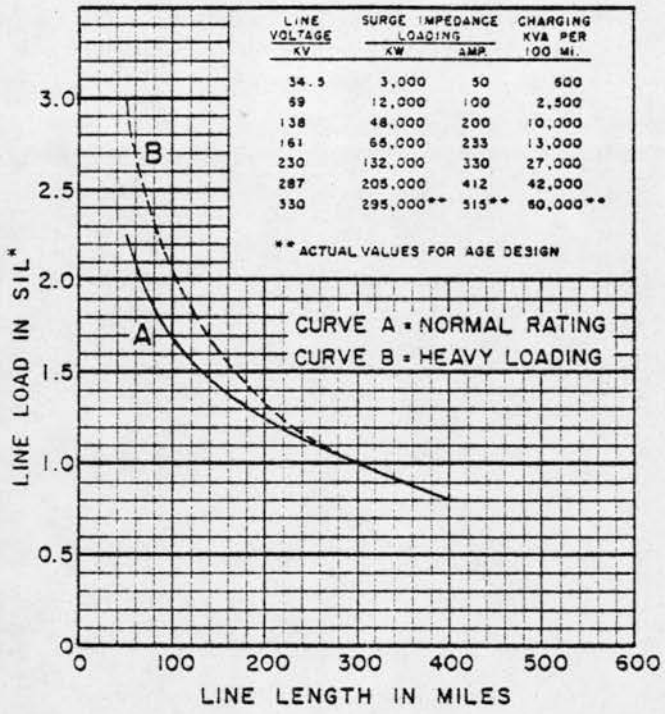

Figure 3.2. St. Clair loadability curve.

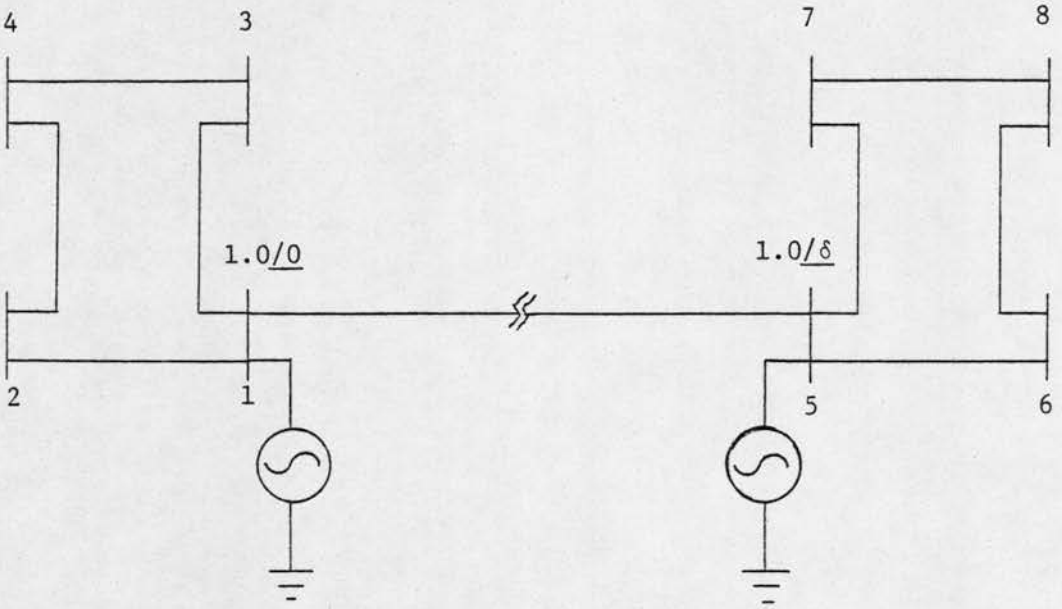

line data:

per unit R per mile = 0.0000571
per unit X per mile = 0.0006432
per unit B per mile = 0.0660400

Figure 3.3. 8-bus 345 kV system.

Since the system of Figure 3.3 is symmetrical, the maximum power transfer of line 1-5 is the same in either direction, so it is only necessary to find the maximum for one direction. To study the maximum power transfer from bus 1 to 5, the generator at bus 5 is outaged and the swing bus provides total system load. With these conditions, the maximum power transfer across the line was found to be 3.53 per unit. The load flow solution with line flows is shown in Figure 3.4. With this maximum power transfer and the operating limit from St. Clair curve, the stability margin is found from Equation (13) to be 28%. This stability margin is acceptable; therefore, the St. Clair limits were sufficiently accurate for this case. The line data used in the load flow are shown in Figure 3.3.

The next system which is studied is shown in Figure 3.5. In this system, a long 400-mile line is sending power to a small 4 bus system. This could be a practical example since power plants are sometimes built in remote areas to serve metropolitan loads. Because of the long line, shunt reactors are included to prevent overvoltages under light loading conditions. It is common practice to leave the shunt reactors connected at all times, so they were included in the model and remained unchanged as the system load was increased. The line data are the same as those shown in Figure 3.3. The shunt susceptance due to line charging is combined in parallel with the shunt reactance at each bus to get a total impedance to ground.

```
**********************************************************************

LOAD FLOW SOLUTION AFTER   6 ITERATIONS

INJECTED POWER AT EACH BUS
 1: P=    6.4934 Q=     .5644
 2: P=    -.5850 Q=     .0000
 3: P=  -1.1700 Q=    -.0000
 4: P=    -.5850 Q=    -.0000
 5: P=     .0007 Q=    1.3592
 6: P=  -1.1700 Q=    0.0000
 7: P=  -1.7550 Q=     .0000
 8: P=    -.5850 Q=    -.0000

LINE FLOWS
 1- 2 P=    1.02966 Q=    -.46060
 1- 3 P=    1.32027 Q=    -.44520
 1- 5 P=    4.14349 Q=    3.12120
 2- 1 P=  -1.02603 Q=     .50152
 2- 4 P=     .44103 Q=    -.16299
 3- 1 P=  -1.31473 Q=     .50763
 3- 4 P=     .14473 Q=    -.16975
 4- 2 P=    -.44041 Q=     .16992
 4- 3 P=    -.14459 Q=     .17131
 5- 1 P=  -3.52886 Q=    3.80231
 5- 6 P=    1.61917 Q=    -.40787
 5- 7 P=    1.91038 Q=    -.38423
 6- 5 P=  -1.61121 Q=     .49754
 6- 8 P=     .44121 Q=    -.16072
 7- 5 P=  -1.89954 Q=     .50635
 7- 8 P=     .14454 Q=    -.17023
 8- 6 P=    -.44060 Q=     .16767
 8- 7 P=    -.14440 Q=     .17181

VOLTAGE PROFILE
V( 1): MAGNITUDE=    .100000E+01  ANGLE=     0.000000
V( 2): MAGNITUDE=    .101246E+01  ANGLE=    -1.948785
V( 3): MAGNITUDE=    .101149E+01  ANGLE=    -2.477974
V( 4): MAGNITUDE=    .101650E+01  ANGLE=    -2.764364
V( 5): MAGNITUDE=    .100000E+01  ANGLE=   -84.128507
V( 6): MAGNITUDE=    .100990E+01  ANGLE=   -87.150361
V( 7): MAGNITUDE=    .100884E+01  ANGLE=   -87.682473
V( 8): MAGNITUDE=    .101387E+01  ANGLE=   -87.970100
```

Figure 3.4. Load flow results for 8-bus system.

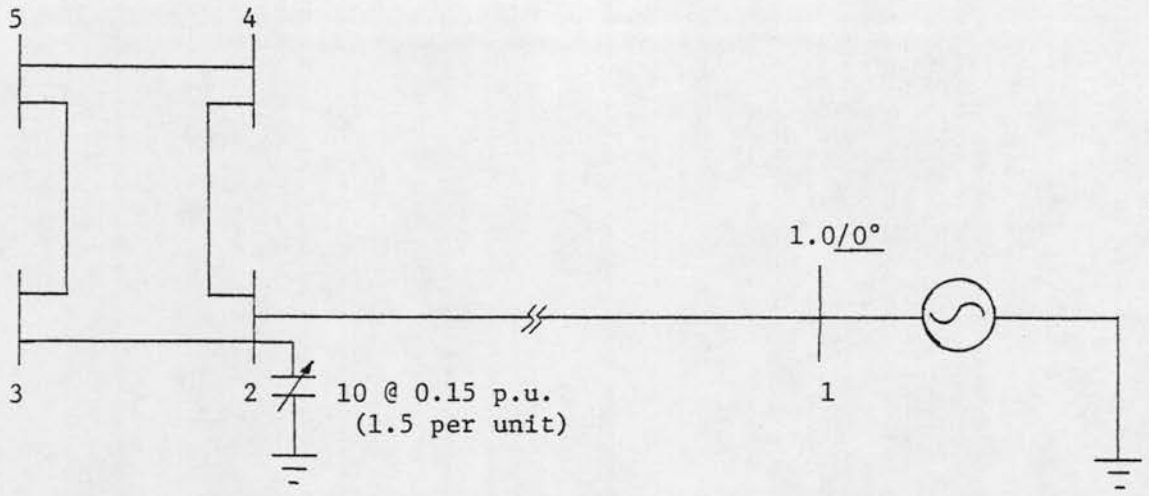

Bus No.	Shunt Reactance

1	
2	0.6448
3	4.343
4	4.343
5	4.343

Figure 3.5. 5-bus 345 kV system.

```
**********************************************************************

LOAD FLOW SOLUTION AFTER   5 ITERATIONS

INJECTED POWER AT EACH BUS
  1: P=    3.1099 Q=     .0465
  2: P=    -.7101 Q=    1.5001
  3: P=    -.7097 Q=    -.0000
  4: P=    -.3549 Q=    -.0000
  5: P=   -1.0646 Q=    -.0000

LINE FLOWS
  1 - 2 P=    3.10988 Q=    1.36737
  2 - 1 P=   -2.84674 Q=    1.60214
  2 - 3 P=     .97951 Q=    -.10195
  2 - 5 P=    1.15714 Q=    -.09253
  3 - 2 P=    -.97651 Q=     .13569
  3 - 4 P=     .26676 Q=    -.04303
  4 - 3 P=    -.26654 Q=     .04557
  4 - 5 P=    -.08833 Q=     .04722
  5 - 2 P=   -1.15298 Q=     .13940
  5 - 4 P=     .08836 Q=    -.04687

VOLTAGE PROFILE
V( 1): MAGNITUDE=    .100000E+01  ANGLE=     0.000000
V( 2): MAGNITUDE=    .961558E+00  ANGLE=   -53.106698
V( 3): MAGNITUDE=    .962628E+00  ANGLE=   -55.075059
V( 4): MAGNITUDE=    .963317E+00  ANGLE=   -55.612751
V( 5): MAGNITUDE=    .962007E+00  ANGLE=   -55.428773
```

Figure 3.6. Load flow results for 5-bus system.

To provide voltage control at the receiving end of the line, 10 shunt capacitors are connected to bus 2. Each capacitor can supply 0.15 per unit reactive power to the system and can be switched in separately. Since the switching steps are very small, it can be assumed that the voltage at bus 2 can be kept constant within a very small tolerance until all of the capacitance is utilized. Therefore, these capacitors are similar to a synchronous condensor with Q_{min} equal to 0 and Q_{max} equal to 1.50.

The loadability found from the St. Clair curve is 2.56 per unit across the 400-mile line. With a 30% stability margin, this would require a maximum power transfer of 3.66 per unit across the line. Since there is a limit on the reactive power which can be supplied by the capacitors, the accuracy of the St. Clair curves might not be acceptable; therefore, it is necessary to look at the system in more detail. The maximum value for the angle across the 400-mile line (δ_{15}) taking into consideration the maximum reactive power of the capacitors can be found using Equations (17) and (18). Both equations must be considered because shunt reactors are used in this system. In these equations, X_{LC} represents the total shunt reactance at bus 2 and X represents the line reactance. The voltage $|\bar{V}_2|$ is fixed at 1.00 until Q_{max} is reached. From Equation (17) it is found that this occurs when δ_{15} is -50.2°. Remember that this is the angle at which the maximum reactive power is reached (all capacitors on line). However, the limit from Equation (18) is -58.1°. Therefore, the maximum power transfer occurs with δ_{15} equal to -58.1°. The power transfer is found by Equation (3) to be 2.89 per unit. It can be seen by comparison that the St. Clair limits are very inaccurate in this case. With a limit of 2.56, the stability margin would be less than 12%.

The results of the load flow, which agrees well with the above predictions, are shown in Figure 3.6. The maximum power transfer occurs when the power flow from bus 1 to bus 5 is 2.85 per unit. It is of interest to note that at the maximum power transfer the voltages are all over 0.95 per unit and all angles are less than 60°, a condition usually considered sufficiently stable.

These two examples show how system parameters can affect the maximum loadability of a transmission line. The same 400-mile line was studied in two systems, in the first, the maximum power transfer was 3.53 per unit and, in the second, 2.85 per unit. The amount of voltage control was the cause of this difference.

As mentioned before and shown by example in this chapter, loadability curves are very useful for lines with good voltage control, but when voltage control is questionable, other methods such as those shown in Chapter 2 must be used to find the maximum power transfer. Since all systems are different, the choice becomes a matter of judgment.

3.4 Actual System Application

In this section, the loadability of one portion of a 345 kV system owned by a western United States utility is studied. The system is shown in Figure 3.7. The data for the system including all series and shunt compensation are shown in Figure 3.8.

The system is studied to find the maximum power transfer capability of the series of lines from bus 1 to bus 5. It is desirable to have a 30% or more stability margin so that under a contingency condition lines from 1 to 5 could supply the extra power necessary.

As indicated in Figure 3.8, the system consists of series compensation, a subject discussed little in the preceding chapters. Series compensation consists of capacitors connected in series along the transmission line. The

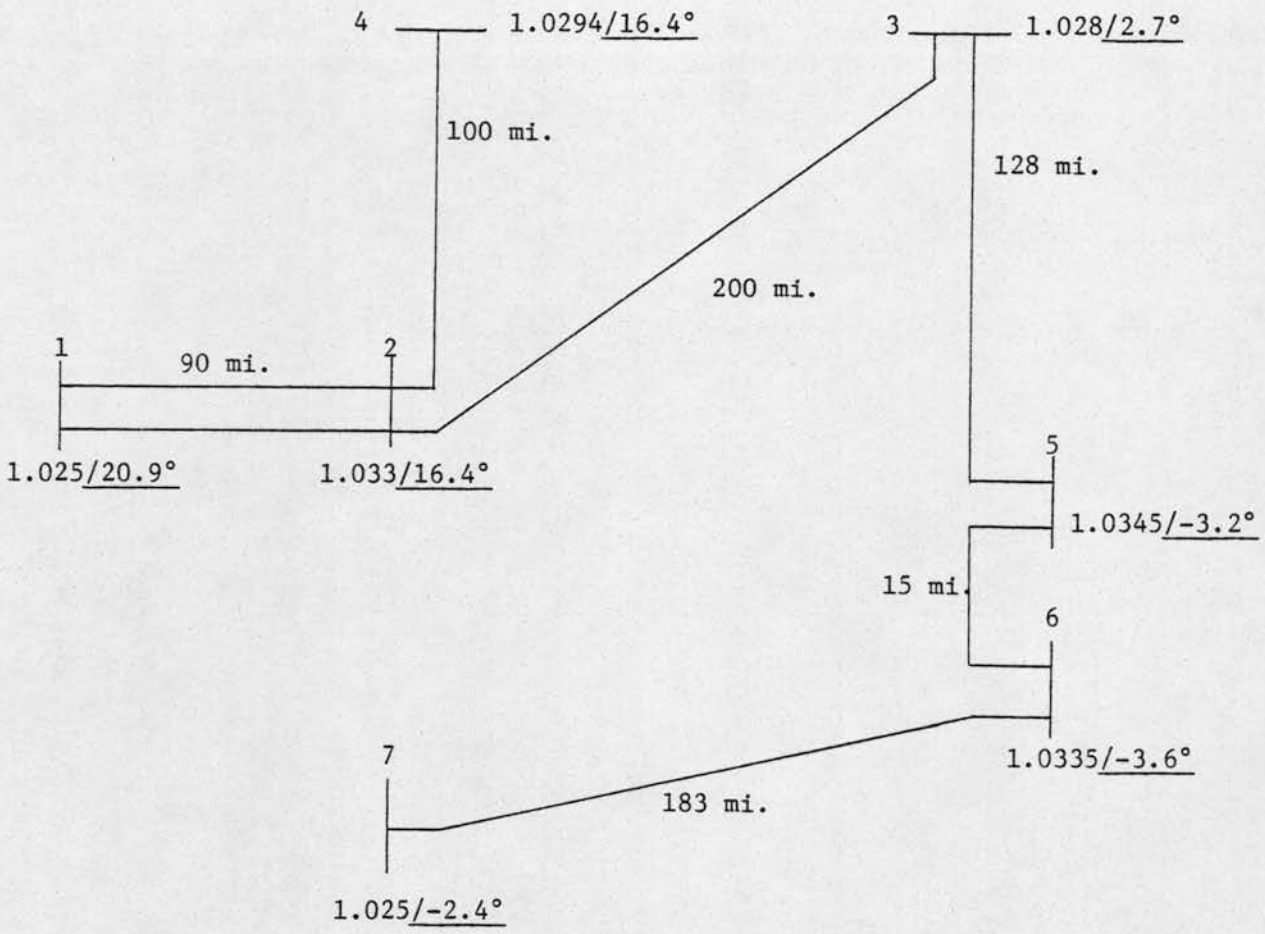

LOAD SCHEDULE UNDER NORMAL OPERATING CONDITIONS

	Load		Shunt		Generation	
Bus	MW	MVAR	MW	MVAR	MW	MVAR
1	0.0	26.2	0.0	-114.5	380.0	0.0
2	100.0	0.0	0.0	-116.3	0.0	0.0
3	95.0	0.0	0.0	-115.2	0.0	0.0
4	0.0	0.0	0.0	- 57.2	0.0	0.0
5	130.6	16.2	0.0	- 57.8	68.0	50.0
6	136.2	9.8	0.0	- 72.6	0.0	0.0
7	0.0	0.0	0.0	- 71.4	25.0	-23.3

Figure 3.7. 7-bus 345 kV system.

Bus #	$X_{C(SHUNT)}$ Line charging	$X_{L(SHUNT)}$ Reactors	$X_{T(SHUNT)}$ Total	Shunt Capacitors
1	-1.273	0.9174	3.284	------
2	-0.473	0.9174	-0.976	------
3	-0.706	0.9174	-3.064	------
4	-2.12	1.835	13.649	------
5	-1.64	1.835	-15.432	8 @ .12 each
6	-1.187	1.470	-6.16	12 @ .12 each
7	-1.275	1.470	-9.6115	------

From	To	R	jX	Series Compensation
1	2	0.0040	0.0434	4 @ 15% each
1	2	0.0040	0.0434	------
2	3	0.0084	0.0916	3 @ 20%
2	4	0.0048	0.0517	------
3	5	0.0057	0.0609	1 @ 40%
5	6	0.0006	0.0065	------
6	7	0.0077	0.0841	------

Figure 3.8. System data for 7-bus 345 kV system.

effect of the series capacitors is to negate a portion of the line reactance and make the line electrically shorter, thus increasing its capacity.

The shunt reactors listed are connected at all times, therefore, they are combined in parallel with the line charging impedance to get an equivalent ground impedance at each bus. The shunt and series capacitors can be switched in separately at any time.

The voltages, generation and load at each bus for normal operating conditions are also shown in Figure 3.7. In order to study the maximum power transfer from bus 1 to bus 5 by the analytical methods described in Chapter 2, an equivalent 2 bus model must be formed. Several approximations must be made to do this; they are listed below.

1. Since bus 4 has no load, line 2-4 does not have any effect on the maximum loadability of 1-5 and can be neglected.
2. Line 6-7 has a negligible effect on the maximum loadability of 1-5 and can be left out.
3. Since buses 5 and 6 are very close, they can be combined into one bus.

With the above approximations made, the system is reduced to that of Figure 3.9. This system can be approximated as a two bus system if the loads at buses 2 and 3 are neglected. Since these loads are small compared with those at buses 5 and 6 combined, this should not make a large difference. If the shunt impedances at buses 3, 5 and 6 are combined in parallel, the system is reduced to a two bus system as shown in Figure 3.10. The maximum power transfer of this line can now be found by the methods described in Chapter 2. Since buses 5 and 6 combined have 20 shunt capacitors rated at 0.12 per unit reactive power each, the receiving end can be modeled as a synchronous condenser with Q_{min} equal to 0 and Q_{max} equal to 2.40.

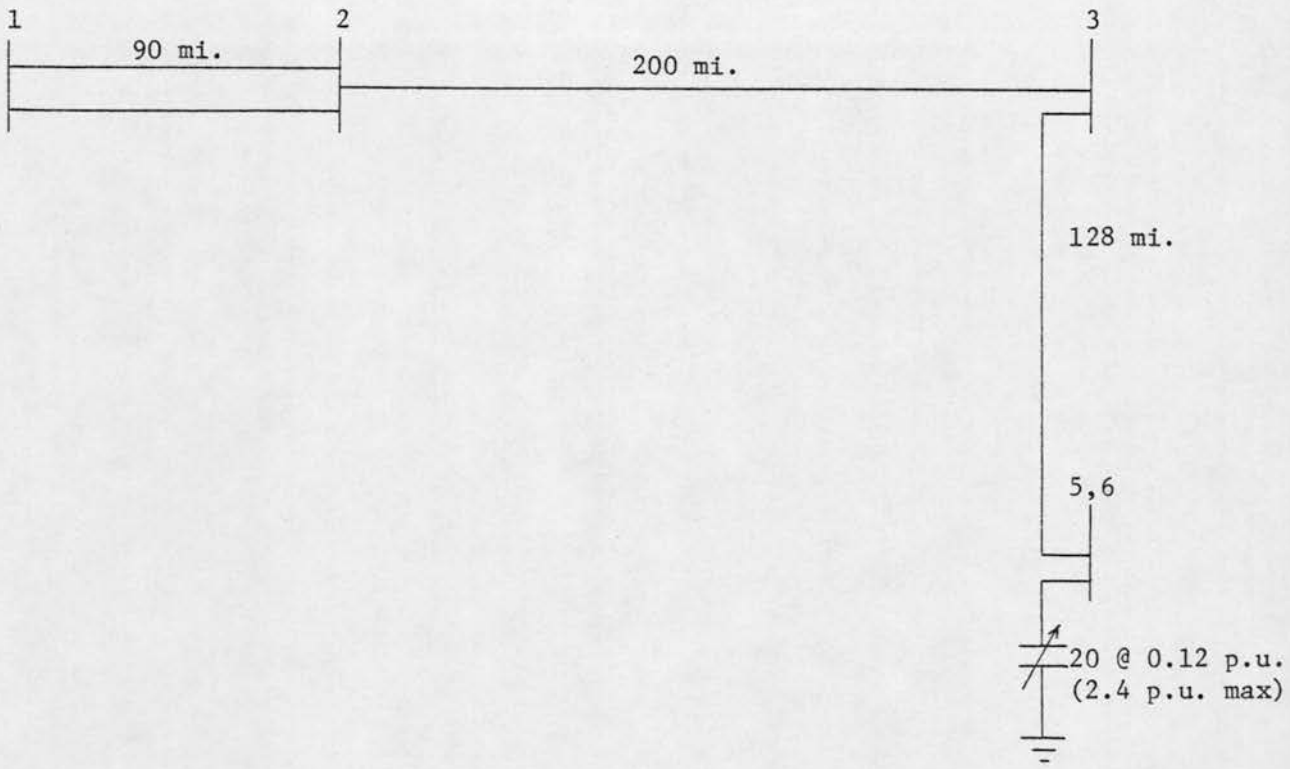

Figure 3.9. 7-bus system after approximations.

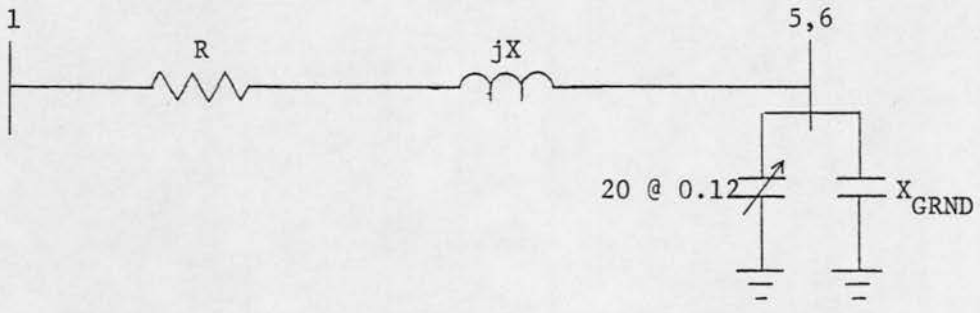

$R = 0.0161$

$X = 0.08558 = X_L - X_C$

$X_{GRND} = -1.806$

Figure 3.10. Two bus approximation of lines 1 to 5.

The line is studied with all series capacitors connected since the maximum power transfer is increased by their addition. However, as mentioned in Chapter 2, when series capacitors and shunt reactors are included in a system, the limits of both Equations (17) and (18) must be found and the largest is the angle of maximum power transfer.

For the line of Figure 3.10, the limit of Equation (17) is -39.85° and the limit of Equation (18) is -52.87°. Therefore, the maximum power transfer should occur when the angle between buses 1 and 5 is 52.87°. Equation (3) can be used to find the power transfer at this angle; however, since the voltage control hits its limit at -39.85°, the voltage $|\bar{V}_5|$ is no longer 1.0345 per unit when δ_{15} is -52.87°. Since the line can be modeled as a constant Q source between -39.85° and -52.87°, the voltage $|\bar{V}_5|$ is given by Equation (21)

$$|\bar{V}_5| = \frac{\frac{|\bar{V}_1|}{X}\cos\delta_{15} + \sqrt{\frac{|V_1|^2}{X^2}\cos^2\delta_{15} + 4X_s Q_{const}}}{2X_s} \qquad (21)$$

where, $X_s = \frac{1}{X_{LINE}} + \frac{1}{X_{GRND}}$

Q_{const} = constant source at bus 5

Equation (21) is derived in Appendix E for the constant Q model. The voltage at $\delta_{15} = -52.87°$ is found to be 0.89. The maximum power transfer can then be found from Equation (3) to be 7.70.

In order to compare this solution with the actual maximum power transfer, the load flow of Figure 3.1 was used on the entire system. At first the loads at buses 2 and 3 were not included and the load at bus 5 was incremented until the load flow failed to converge. The maximum occurred when the power transfer to bus 5 was 7.68 and the angle from bus 1 to 5 was -56.43°. This agrees well with the above values of 7.70 and -52.87°.

The load flow was run a second time with the loads at buses 2 and 3 included. The maximum power transfer from bus 1 to bus 5 is reduced to 7.21. The stability margin will decrease by about 5% with the intermediate loads included, therefore, this must be compensated for when the stability margin is chosen. If a stability margin greater than or equal to 35% is chosen, the loads at buses 2 and 3 will not have a great effect unless they become a much larger percentage of the load at bus 5. The results for the load flows without and with intermediate loads are shown in Figures 3.11 and 3.12, respectively.

```
**********************************************************************
LOAD FLOW SOLUTION AFTER   7 ITERATIONS

INJECTED POWER AT EACH BUS
 1: P=    9.4015 Q=    4.3500
 2: P=    -.0002 Q=     .0000
 3: P=    -.0003 Q=     .0001
 4: P=    -.0000 Q=    -.0000
 5: P=   -2.7327 Q=     .9600
 6: P=   -5.9487 Q=    1.4400
 7: P=    1.0720 Q=    1.9000

LINE FLOWS
 1- 2 P=    9.40147 Q=    4.03004
 2- 1 P=   -9.16633 Q=   -2.79042
 2- 3 P=    9.16609 Q=    3.66771
 2- 4 P=     .00002 Q=     .06729
 3- 2 P=   -8.27798 Q=     .20616
 3- 5 P=    8.27767 Q=     .00560
 4- 2 P=    -.00000 Q=    -.06703
 5- 3 P=   -7.67544 Q=    3.85503
 5- 6 P=    4.94273 Q=   -2.84983
 6- 5 P=   -4.91475 Q=    3.15286
 6- 7 P=   -1.03399 Q=   -1.59416
 7- 6 P=    1.07200 Q=    2.00934

VOLTAGE PROFILE
V( 1): MAGNITUDE=    .102500E+01  ANGLE=     0.000000
V( 2): MAGNITUDE=    .960149E+00  ANGLE=    -6.271751
V( 3): MAGNITUDE=    .805311E+00  ANGLE=   -29.507398
V( 4): MAGNITUDE=    .956526E+00  ANGLE=    -6.251677
V( 5): MAGNITUDE=    .835614E+00  ANGLE=   -56.215276
V( 6): MAGNITUDE=    .855192E+00  ANGLE=   -58.929369
V( 7): MAGNITUDE=    .102500E+01  ANGLE=   -54.041760
```

Figure 3.11. Load flow results with no intermediate loads.

```
**********************************************************************
LOAD FLOW SOLUTION AFTER   7 ITERATIONS

INJECTED POWER AT EACH BUS
 1: P=   11.0676 Q=    5.0822
 2: P=   -1.0014 Q=     .0000
 3: P=    -.9514 Q=     .0002
 4: P=    -.0000 Q=     .0000
 5: P=   -2.5675 Q=     .9599
 6: P=   -5.5886 Q=    1.4399
 7: P=    1.0070 Q=    1.9149

LINE FLOWS
 1- 2 P=   11.06760 Q=    4.76223
 2- 1 P=  -10.74135 Q=   -3.04228
 2- 3 P=    9.73990 Q=    3.90066
 2- 4 P=     .00002 Q=     .06583
 3- 2 P=   -8.71474 Q=     .57099
 3- 5 P=    7.76335 Q=    -.36685
 4- 2 P=    -.00000 Q=    -.06559
 5- 3 P=   -7.21244 Q=    3.89850
 5- 6 P=    4.64491 Q=   -2.89352
 6- 5 P=   -4.61907 Q=    3.17342
 6- 7 P=    -.96954 Q=   -1.61508
 7- 6 P=    1.00700 Q=    2.02425

VOLTAGE PROFILE
V( 1): MAGNITUDE=   .102500E+01 ANGLE=     0.000000
V( 2): MAGNITUDE=   .949729E+00 ANGLE=    -7.467972
V( 3): MAGNITUDE=   .790549E+00 ANGLE=   -33.042627
V( 4): MAGNITUDE=   .946145E+00 ANGLE=    -7.447898
V( 5): MAGNITUDE=   .833943E+00 ANGLE=   -58.730310
V( 6): MAGNITUDE=   .854013E+00 ANGLE=   -61.299832
V( 7): MAGNITUDE=   .102500E+01 ANGLE=   -56.771992
```

Figure 3.12. Load flow results with intermediate loads.

The St. Clair curve can also be used to predict the loadability of the line from bus 1 to bus 5. Since the St. Clair curve uses length, it is necessary to get an equivalent length of the line. Using a base reactance of 0.00046 per unit per mile found using the 200 mile line from bus 2 to bus 3, the approximate length of the line of Figure 3.10 is 180 miles. The limit of a line of 180 miles from the St. Clair curve of Figure 3.2 is 1.3 SIL

or 5.07 per unit. A surge impedance loading of 390 MW is used instead of 320 MW since the lines are in two conductor bundles. These values of surge impedance loadings are given in reference [3]. This limit gives a stability margin of around 35% which is acceptable; however, the St. Clair curves are not guaranteed to give accurate results for lines with series capacitors since series compensation affects line reactance but does not affect line charging; therefore, the line is not truly reduced in length. The results for this system were probably good because shunt reactors were also used. Loadability curves could be derived for lines with specific series compensation levels but none have been published. The reader is referred to reference [3] for more information on this topic.

If this system were to be studied by linear programming techniques, the limit on line 3-5 would be set at 7.70 per unit since the load on this line represents the power transferred from bus 1 to bus 5. If loads are included at buses 2 and 3, the line flows of 1 to 2 and 2 to 3 will be somewhat higher, but unless these loads become substantially higher, to limit the power transfer of one of these lines, the maximum power transfer from 1 to 5 will not be greatly changed.

It should be noted that the power transfer from bus 1 to bus 5 was found analytically only after several approximations were made. It is obvious that as the system in study becomes more complex it may not be possible to get an accurate two bus model, therefore, the accuracy of linear programs for these systems becomes increasingly questionable.

4. CONCLUSIONS AND RECOMMENDATIONS

The objective of this thesis was to define an accurate way to find the maximum power transfer of a transmission line. These limits would then be used in linear programs to find the maximum loadability of a system.

The classic St. Clair curves and more recent loadability curves were tested for their accuracy. It was found that these curves give accurate results for transmission lines in systems with very strong voltage control. Consequently, it was discovered that the amount of voltage control is most often the determining factor in line loadability.

The maximum power transfer of a single line with limited voltage control was studied in detail and a comparison was made between shunt static capacitors and synchronous condensers. For a single line model with a synchronous condenser of some maximum capacity, the maximum stability angle was found analytically as a function of the maximum capacity and other line parameters. It was noted that a static capacitor with small switching steps could be modeled as a synchronous condenser in order to find the maximum stability angle.

Systems were studied which showed where the St. Clair curves give accurate results and where they do not. Where they don't, the analytical method of Chapter 2 was applied.

Many questions arise when the loadability of more complex systems are studied. If the voltage control is good throughout the entire system, the St. Clair limits will be accurate. Linear programs could be used and the maximum power transfer found. However, if the voltage control in any one part of the system is weak, there is no insurance that the linear program will give accurate results.

It was also found that the analytical solutions of Chapter 2 might be impossible to apply to complex systems since it is based on a single line model. Therefore, it is the opinion of this author that for complex systems with areas of weak voltage control further study is needed to find the maximum power transfer of the system without using costly load flows.

REFERENCES

[1] E. Clarke and S. B. Crary, "Stability limitations of long distance A-C power-transmission systems," AIEE Trans., vol. 60, pp. 1051-1059, 1941.

[2] H. P. St. Clair, "Practical concepts in capability and performance of transmission lines," AIEE Trans., vol. 72, pp. 1152-1157, 1953.

[3] R. D. Dunlop, R. Gutman, P. P. Marchenko, "Analytical development of loadability characteristics for EHV and UHV transmission lines," IEEE Trans. Power Apparatus and Systems, vol. PAS-98, no. 2, pp. 606-677, 1979.

[4] S. Linke, "Surge-impedance loading and power-transmission capability revisited," Paper no. A77-249-6, IEEE Trans., vol. PAS-96, no. 4, p. 1079, July/August, 1977. Full text in IEEE Publication 77CH1190-8-PWR, 1977.

[5] Glenn W. Stagg and Ahmed H. El-Abiad, Computer Methods in Power System Analysis. New York: McGraw-Hill, 1968.

[6] L. L. Garver, P. R. Van Horne and K. A. Wirgau, "Load supplying capability of generation-transmission networks," IEEE Trans. Power Apparatus and Systems, vol. PAS-98, no. 3, May/June 1979.

[7] P. W. Sauer, "On the formulation of power distribution factors," Paper 80SM614-8. Presented at 1980 PES Summer Meeting, Minneapolis, MN, July 13-18, 1980.

[8] B. K. Johnson, "Extraneous and false load flow solutions," IEEE Trans. Power Apparatus and Systems, vol. PAS-96, no. 2, March/April, 1977.

[9] W. A. Johnson, J. F. Aldrich, R. A. Fernandes, H. H. Happ, K. A. Wirgau, R. P. Schulte, W. R. Bosshard, J. D. Willson, R. E. Reed, "EHV operating problems associated with reactive control," IEEE Publication 80SM513-2, 1980.

[10] J. Kekela and L. Firestone, "Underexcited operation of generators," IEEE Publication CP-63-1403, 1963.

[11] T. J. Nagel and G. S. Vassell, "Basic principles of planning var control on the American electric power systems," IEEE Publication 31PP66-509, 1966.

APPENDIX A

SURGE IMPEDANCE LOADING

The surge impedance (or characteristic impedance) of a transmission line is defined as $\sqrt{L/C}$, where L is the inductance of the line and C is the capacitance.

The surge impedance loading of a line is defined in Equation (22).

$$SIL = \frac{(KV_{L-L})^2}{\text{Surge impedance}} \qquad (22)$$

If a unity power factor load equal to the surge impedance loading is located at the receiving end of a line, the reactive power lost in the inductance of the line is equal to the reactive power supplied by line charging.

When using the loadability curves, it is advantageous to use surge impedance loading because then the same curve could be used for several different voltages.

APPENDIX B

ANALYTICAL DERIVATION OF LOADABILITY CURVES

In this section, an analytical derivation of equations used in forming the loadability curves is shown. In the following equations, (.)* denotes conjugation.

The injected power at each node is given by Equations (23)-(26), as shown in Figure 1.2.

$$\bar{S}_1 = |V_1|\underline{/\delta_1}[\bar{Y}^*_{11}|V_1|\underline{/-\delta_1} + \bar{Y}^*_{12}|\bar{V}_2|\underline{/-\delta_2}] \tag{23}$$

$$\bar{S}_2 = 0 = |\bar{V}_2|\underline{/\delta_2}[\bar{Y}^*_{21}|\bar{V}_1|\underline{/-\delta_1} + \bar{Y}^*_{22}|\bar{V}_2|\ \underline{/-\delta_2} + \bar{Y}^*_{23}|\bar{V}_3|\underline{/-\delta_3}] \tag{24}$$

$$\bar{S}_3 = 0 = |\bar{V}_3|\underline{/\delta_3}[\bar{Y}^*_{32}|\bar{V}_2|\underline{/-\delta_2} + \bar{Y}^*_{33}|\bar{V}_3|\underline{/-\delta_3} + \bar{Y}^*_{34}|\bar{V}_4|\underline{/0°}] \tag{25}$$

$$\bar{S}_4 = |\bar{V}_4|\underline{/0°}[\bar{Y}^*_{43}|\bar{V}_3|\underline{/-\delta_3} + \bar{Y}^*_{44}|\bar{V}_4|\underline{/0°}] \tag{26}$$

In the above equations the unknowns are $|\bar{V}_1|$, $|\bar{V}_3|$, δ_2, δ_3. Equations (24) and (25) can be rewritten as (27) and (28).

$$0 = \bar{Y}^*_{21}|\bar{V}_1|\underline{/-\delta_1} + \bar{Y}^*_{22}|\bar{V}_2|\underline{/-\delta_2} + \bar{Y}^*_{23}\ \bar{V}^*_3 \tag{27}$$

$$0 = \bar{Y}^*_{32}|\bar{V}_2|\ \underline{/-\delta_2} + \bar{Y}^*_{33}\ \bar{V}^*_3 + \bar{Y}^*_{34}|\bar{V}_4|\underline{/0°} \tag{28}$$

Equation (28) can be solved for $\bar{V}^*_3$ to give Equation (29).

$$\bar{V}^*_3 = (-\bar{Y}^*_{32}|\bar{V}_2|\underline{/-\delta_2} - \bar{Y}^*_{34}|\bar{V}_4|\underline{/0°})/\bar{Y}^*_{33} \tag{29}$$

This value for $\bar{V}^*_3$ can be substitute into Equation (27) to give Equation (30).

$$0 = \bar{Y}^*_{21}|\bar{V}_1|\underline{/-\delta_1} + \bar{Y}^*_{22}|\bar{V}_2|/-\delta_2 - \frac{\bar{Y}^*_{23}\ \bar{Y}^*_{32}}{Y^*_{33}}\ |\bar{V}_2|\underline{/-\delta_2} - \frac{\bar{Y}^*_{34}\ \bar{Y}^*_{23}}{\bar{Y}^*_{33}}|\bar{V}_4|\underline{/0°} \tag{30}$$

The real part of Equation (30) is taken; this is shown in Equation (31) after simplifying

$$0 = |\bar{Y}_{21}| \cos(-\delta_1 - \theta_{21})|\bar{V}_1|$$
$$+ \left[|\bar{Y}_{22}||\bar{V}_2| \cos \theta_{22} - \frac{|\bar{Y}_{23}||\bar{Y}_{32}|}{|\bar{Y}_{33}|} \cos (\theta_{23} + \theta_{32} - \theta_{33}) \right] \cos \delta_2$$
$$+ \left[\frac{|\bar{Y}_{23}||\bar{Y}_{32}|}{|\bar{Y}_{33}|} \sin (\theta_{23} + \theta_{32} - \theta_{33}) - |\bar{Y}_{22}||\bar{V}_2| \sin \theta_{22} \right] \sin \delta_2$$
$$- \frac{|\bar{Y}_{34}||\bar{Y}_{32}|}{|\bar{Y}_{33}|} |\bar{V}_4| \cos (-\theta_{34} - \theta_{23} + \theta_{33}) \qquad (31)$$

To simplify this equation, the coefficients are redefined as C_1, C_2, C_3 and C_4. The result is shown in Equation (32).

$$0 = C_1|\bar{V}_1| + C_2 \cos \delta_2 + C_3 \sin \delta_2 + C_4 \qquad (32)$$

The imaginary part of Equation (30) is taken and after a similar procedure Equation (33) is obtained.

$$0 = B_1|\bar{V}_1| + B_2 \cos \delta_2 + B_3 \sin \delta_2 + B_4 \qquad (33)$$

The coefficients of Equation (33) are defined below.

$$B_1 = |\bar{Y}_{21}| \sin(-\delta_1 - \theta_{21}) \qquad (34)$$

$$B_2 = \frac{|\bar{Y}_{23}||\bar{Y}_{32}||\bar{V}_2|}{|\bar{Y}_{33}|} \sin (\theta_{23} + \theta_{32} - \theta_{33}) - |\bar{Y}_{22}||\bar{V}_2| \sin \theta_{22} \qquad (35)$$

$$B_3 = \frac{|\bar{Y}_{23}||\bar{Y}_{32}||\bar{V}_2|}{|\bar{Y}_{33}|} \cos (\theta_{23} + \theta_{32} - \theta_{33}) - |\bar{Y}_{22}||\bar{V}_2| \cos \theta_{22} \qquad (36)$$

$$B_4 = - \frac{|\bar{Y}_{34}||\bar{Y}_{23}||\bar{V}_4|}{|\bar{Y}_{33}|} \sin (-\theta_{34} - \theta_{23} + \theta_{33}) \qquad (37)$$

Equation (32) can now be solved for $|\bar{V}_1|$.

$$|\bar{V}_1| = -\frac{C_2}{C_1}\cos\delta_2 - \frac{C_3}{C_1}\sin\delta_2 - \frac{C_4}{C_1} \tag{38}$$

This equation is then substituted into Equation (33) to give:

$$0 = \left[B_2 - \frac{B_1C_2}{C_1}\right]\cos\delta_2 + \left[B_3 - \frac{B_1C_3}{C_1}\right]\sin\delta_2 + \left[B_4 - \frac{B_1C_4}{C_1}\right] \tag{39}$$

Equation (39) can now be solved for δ_2.

$$\delta_2 = \cos^{-1}\left[\frac{-D_3}{\sqrt{D_1^2 + D_2^2}}\right] + \tan^{-1}\left(\frac{D_2}{D_1}\right) \tag{40}$$

The coefficients of Equation (40) are shown below.

$$D_1 = B_2 - \frac{B_1C_2}{C_1} \tag{41}$$

$$D_2 = B_3 - \frac{B_1C_3}{C_1} \tag{42}$$

$$D_3 = B_4 - \frac{B_1C_4}{C_1} \tag{43}$$

Once δ_2 is obtained, $|\bar{V}_1|$ can be found by Equation 38 and $\bar{V}_3$ by Equation (29). The whole system is then solved.

APPENDIX C

LOADABILITY OF A SINGLE LINE WITH CONSTANT POWER FACTOR LOAD

In this section, Equations (9) to (14) of Chapter 2 are proved. Figure 2.3 is referred to and a shunt capacitor is included at bus 2. For the solution with no shunt capacitor, B is set equal to 0 in the following equations.

The real and reactive power delivered to the load at bus 2 is given by Equations (44) and (45) below.

$$P = - \frac{|\bar{V}_1||\bar{V}_2|}{X} \sin \delta \tag{44}$$

$$Q = \frac{|\bar{V}_1||\bar{V}_2|}{X} \cos \delta + (B - \frac{1}{X})|\bar{V}_2|^2 \tag{45}$$

Since the power factor is constant, Q is related to P by Equation (46):

$$Q = \left(\frac{RPF}{PF}\right)P \tag{46}$$

Equation (46) is then substituted into Equation (45). After simplifying, Equation (47) results.

$$|\bar{V}_2|(BX - 1) + |\bar{V}_1|(\cos \delta + \left(\frac{RPF}{PF}\right) \sin \delta) = 0 \tag{47}$$

Equation (47) can easily be solved for $|\bar{V}_2|$:

$$|\bar{V}_2| = - \frac{|\bar{V}_1|}{(BX - 1)}\left[\cos \delta + \left(\frac{RPF}{PF}\right) \sin \delta\right] \tag{48}$$

The derivative of $|\bar{V}_2|$ with respect to δ is taken:

$$\frac{d|\bar{V}_2|}{d\delta} = \frac{-|\bar{V}_1|}{(BX - 1)} \left[-\sin \delta + \left(\frac{RPF}{PF}\right)\cos \delta\right] \tag{49}$$

The maximum power transfer occurs when the derivative of P with respect to δ is 0. This derivative is given in Equation (50).

$$\frac{dP}{d\delta} = \frac{-|\bar{V}_1|}{X}\left[\frac{d|\bar{V}_2|}{d\delta}\right] \sin \delta - \frac{|\bar{V}_1||\bar{V}_2|}{X} \cos \delta \qquad (50)$$

Equations (48) and (49) are substituted into Equation (50) and this equation is set equal to 0. After some algebraic manipulation, this results in Equation (51).

$$\tan \delta - \cot \delta = 2\left(\frac{RPF}{PF}\right) \qquad (51)$$

This equation gives the angle of maximum power transfer.

APPENDIX D

STABILITY LIMIT OF A SINGLE LINE WITH A SYNCHRONOUS CONDENSER AT RECEIVING END

Equation (17) of Chapter 2 is proved here. Figure 2.3 is again referred to, except this time a synchronous condenser is located at bus 2 instead of a static capacitor. The synchronous condenser has some maximum capacity Q_{max} and keeps the voltage $|\bar{V}_2|$ at a specified value until Q_{max} is reached. It is desired to find at what angle of δ this occurs.

The real power delivered to the load is the same as Equation (44) of Appendix C. The reactive power to the load is given in Equation (52).

$$Q = \frac{|\bar{V}_1||\bar{V}_2|}{X} \sin(\delta + 90°) - |\bar{V}_2|^2\left(\frac{1}{X} + \frac{1}{X_{LC}}\right) + Q_{SC} \tag{52}$$

In Equation (52), X_{LC} is the reactance due to line charging at bus 2. Q_{SC} is the reactive power supplied by the synchronous condenser. When the synchronous condenser first hits its limit, the voltage $|\bar{V}_2|$ will still be at its specified value; therefore, at the instant Q_{max} is reached, Equation (52) could be solved with $|\bar{V}_2|$ at its specified limit to give the angle δ at that point. For simplicity, only unity power factor loads were studied. This makes Q equal to 0 in Equation (52).

Equation (52) can now be solved with Q equal to 0, Q_{SC} equal to Q_{max} and the and the voltages equal to their fixed values. The result is shown in Equation (53).

$$\delta = \cos^{-1}\left[\frac{|\bar{V}_2|^2\left(\frac{1}{X} + \frac{1}{X_{LC}}\right) - Q_{max}}{\frac{|\bar{V}_1||\bar{V}_2|}{X}}\right] \tag{53}$$

This equation gives the angle at the instant Q_{max} is reached.

APPENDIX E

STABILITY LIMIT OF A SINGLE LINE WITH A CONSTANT REACTIVE SOURCE AT THE RECEIVING END

The maximum stability angle for the system in Figure 2.3 with a constant reactive source at bus 2 is found in this section. Constant reactive source means that the injected reactive power at bus 2 is the same throughout all levels of load.

The equation for reactive power to the load is the same as Equation (52) in Appendix D except that Q_{SC} is constant. This is referred to as Q_{const} in this section. For simplicity, only unity power factor loads are considered. Equation (52) is then revised to

$$0 = \frac{|\bar{V}_1||\bar{V}_2|}{X} \cos \delta - |\bar{V}_2|^2 X_S + Q_{const} \tag{54}$$

symbols: $X_S = \left(\frac{1}{X} + \frac{1}{X_{LC}}\right)$

In order to find the maximum stability angle, equations for $|\bar{V}_2|$ and the derivative of $|\bar{V}_2|$ with respect to δ are necessary. These equations are used to find where the derivative of P with respect to δ is 0 (Equation (50)). This is the maximum power transfer. The value $|\bar{V}_2|$ can be solved for from Equation (54).

$$|\bar{V}_2| = \frac{\frac{|\bar{V}_1|}{X} \cos \delta \pm [T]^{1/2}}{2X_S} \tag{55}$$

where

$$T = \frac{|\bar{V}_1|^2}{X^2} \cos^2 \delta + 4X_S Q_{const} \quad . \tag{56}$$

Since $|\bar{V}_2|$ must be positive, the plus sign gives the correct answer in Equation (55). The next step is to find the derivative of $|\bar{V}_2|$ with Respect to δ. After some manipulation, the result is given in Equation (57).

$$\frac{d|\bar{V}_2|}{d\delta} = - \frac{|\bar{V}_1|}{2XX_S} \sin \delta \left[1 + \frac{\frac{\bar{V}_1}{X} \cos \delta}{[T]^{1/2}} \right] \tag{57}$$

Equations (55) and (57) can now be substituted into Equation (50) to find the angle of maximum power transfer. After some manipulation and trigonometric identities, the result is Equation (58).

$$\frac{|\bar{V}_1|^2}{X2} \tan^4 \delta - 4X_S Q_{const} \tan^2 \delta - \left[4X_S Q_{const} + \frac{|\bar{V}_1|^2}{X^2} \right] = 0 \tag{58}$$

Note that this equation is a quadratic of $\tan^2 \delta$, which is solved for and shown in Equation (59).

$$\tan^2 \delta = \frac{4X_S Q_{const} + \sqrt{16X_S^2 Q_{const}^2 + 4 \frac{|\bar{V}_1|^2}{X^2} \left(4X_S Q_{const} + \frac{|\bar{V}_1|^2}{X^2} \right)}}{2 \frac{|\bar{V}_1|^2}{X^2}} \tag{59}$$

The value of δ can be easily solved for by Equation (59) and the result is shown in Equation (60).

$$\delta_{max} = \tan^{-1} \left[\frac{4X_S Q_{const} + \sqrt{16 X_S^2 Q_{const}^2 + \frac{4|\bar{V}_1|^2}{X^2} \left(4X_S Q_{const} + \frac{|\bar{V}_1|^2}{X^2} \right)}}{\frac{2|\bar{V}_1|^2}{X^2}} \right]^{1/2} \tag{60}$$

APPENDIX F

PROGRAM LISTINGS

The following pages are listings of two digital computer programs written for use on a CDC CYBER 170.

The program used to reproduce the St. Clair curve as derived in Appendix B is shown on pages 52 thru 54.

The load flow used in Chapter 3 begins on page 55.

```
      PROGRAM LOAD(INPUT,OUTPUT,TAPE5=INPUT,TAPE6=OUTPUT)
      REAL C1,C2,C3,C4,B1,B2,B3,B4,D1,D2,D3,
     +V(4),DELT(4),THETA(4,4)
      COMPLEX ZLL,ZL,B,Y(4,4),V2,V3,SL,S1,V1,ZT
      INTEGER MILES
      DO 1 L=1,4
      DO 1 M=1,4
      Y(L,M)=(0.0,0.0)
1     CONTINUE
      V(4)=0.98
      DELT(4)=0.0
      DELT(1)=0.0175
      MILES=50
      DO 15 K=1,50
      READ(5,10)I,J,ZLL
10    FORMAT(2I1,2F8.5)
      IF(I.EQ.0)GO TO 20
      ZT=ZLL
      Y(I,I)=Y(I,I)+1/ZLL
      Y(J,J)=Y(J,J)+1/ZLL
      Y(I,J)=Y(I,J)-1/ZLL
      Y(J,I)=Y(J,I)-1/ZLL
15    CONTINUE
20    READ(5,25)B,ZL
25    FORMAT(2F8.5,2F10.7)
26    Y(2,2)=Y(2,2)+(B*MILES/2)+1/(ZL*MILES)
      Y(3,3)=Y(3,3)+(B*MILES/2)+1/(ZL*MILES)
      Y(2,3)=Y(2,3)-1/(ZL*MILES)
      Y(3,2)=Y(3,2)-1/(ZL*MILES)
      DO 30 M=1,4
      DO 35 N=1,4
      IF(ABS(REAL(Y(M,N))).LT.1E-10)GO TO 40
      IF(ABS(AIMAG(Y(M,N))).LT.1E-10)GO TO 45
      THETA(M,N)=ATAN2(AIMAG(Y(M,N)),REAL(Y(M,N)))
      GO TO 35
40    IF(AIMAG(Y(M,N)).GT.0)THETA(M,N)=3.14/2
      IF(AIMAG(Y(M,N)).LT.0)THETA(M,N)=-3.14/2
      IF(ABS(AIMAG(Y(M,N))).LT.1E-10)THETA(M,N)=0.0
      GO TO 35
45    THETA(M,N)=0.0
```

```
 35     CONTINUE
 30     CONTINUE
        DO 42 J=1,4
        DO 42 K=1,4
        WRITE(6,47)Y(J,K),THETA(J,K)
 47     FORMAT(1H0,F10.5,2X,F10.5,5X,F10.5)
 42     CONTINUE
 41     C1=CABS(Y(2,1))*COS(-DELT(1)-THETA(2,1))
        C2=CABS(Y(2,2))*COS(THETA(2,2))
       /-CABS(Y(2,3)*Y(3,2)/Y(3,3))
       /*COS(THETA(2,3)+THETA(3,2)-THETA(3,3))
        C3=CABS(Y(2,3)*Y(3,2)/Y(3,3))
       /*SIN(THETA(2,3)+THETA(3,2)-THETA(3,3))
       /-CABS(Y(2,2))*SIN(THETA(2,2))
        C4=-CABS(Y(3,4)*Y(2,3)/Y(3,3))*V(4)
       /*COS(-THETA(3,4)-THETA(2,3)+THETA(3,3))
        B1=CABS(Y(2,1))*SIN(-DELT(1)-THETA(2,1))
        B2=CABS(Y(2,3)*Y(3,2)/Y(3,3))
       /*SIN(THETA(2,3)+THETA(3,2)-THETA(3,3))
       /-CABS(Y(2,2))*SIN(THETA(2,2))
        B3=CABS(Y(2,3)*Y(3,2)/Y(3,3))
       /*COS(THETA(2,3)+THETA(3,2)-THETA(3,3))
       /-CABS(Y(2,2))*COS(THETA(2,2))
        B4=-CABS(Y(3,4)*Y(2,3)/Y(3,3))*V(4)
       /*SIN(-THETA(3,4)-THETA(2,3)+THETA(3,3))
        A=COS(DELT(1))
        F=SIN(DELT(1))
        V1=CMPLX(A,F)
        D1=C2*(B1+B4)-B2*(C1+C4)
        D2=C3*(B1+B4)-B3*(C1+C4)
        DELT(2)=ATAN(-D1/D2)
        V(2)=-(C1+C4)/(C2*COS(DELT(2))+C3*SIN(DELT(2)))
        R=V(2)*COS(DELT(2))
        G=V(2)*SIN(DELT(2))
        V2=CMPLX(R,G)
        V3=(-Y(3,2)*V2-Y(3,4)*V(4))/Y(3,3)
        V(3)=CABS(V3)
        DELT(3)=ATAN(AIMAG(V3)/REAL(V3))
        SL=V3*((CONJG(V2)-CONJG(V3))/(CONJG(ZL)*MILES))
        PL=REAL(SL)
```

```
      QL=AIMAG(SL)
      DELT1=DELT(1)*180./3.14
      DELT2=DELT(2)*180./3.14
      DELT3=DELT(3)*180./3.14
      S1=V1*((CONJG(V1)-CONJG(V2))/CONJG(ZT))
      P1=REAL(S1)
      Q1=AIMAG(S1)
      WRITE(6,51)MILES,DELT1,DELT2,V(3),DELT3,SL,P1,V(2)
51    FORMAT(1HO,2HM=,I3,3X,3HD1=,F9.5,3X,3HD2=,F9.5,
     +3X,3HV3=,F8.5,3X,3HD3=,F9.5,3X,3HSL=,F10.5,2X,F10.5,2X,3HP1=,
     +F10.5,2X,3HV2=,F10.5)
      DELT(1)=DELT(1)+0.0175
      IF(V(3).LT.0.94)GO TO 55
      IF(DELT(1).LT.0.7680)GO TO 41
      WRITE(6,44)
44    FORMAT(1HO,18HLIMIT BY STABILITY)
      WRITE(6,50)MILES,PL,QL
50    FORMAT(1HO,I3,3X,F10.5,3X,F10.5)
      GO TO 65
55    WRITE(6,60)
60    FORMAT(1HO,21HLIMIT BY VOLTAGE DROP)
      WRITE(6,50)MILES,PL,QL
65    Y(2,2)=Y(2,2)-(B*MILES/2)-1/(ZL*MILES)
      Y(3,3)=Y(3,3)-(B*MILES/2)-1/(ZL*MILES)
      Y(2,3)=Y(2,3)+1/(ZL*MILES)
      Y(3,2)=Y(3,2)+1/(ZL*MILES)
      DELT(1)=0.0175
      MILES=MILES+50
      IF(MILES.LE.600)GO TO 26
      STOP
      END
```

```
      PROGRAM MAIN(INPUT,OUTPUT,TAPE5=INPUT,TAPE6=OUTPUT)
      INTEGER BUS(5),NODE,B1,B2,CODE,FLAG,ELIM,GBUS,NCODE(12)
     +,UNT(12),UKNT(12)
      COMPLEX TF(12,12),Y(12,12),ZL,LTOT,Z(12,12),ZLU(12,12)
     +,YLU(12,12),P(12,12),S(12),ST
     +,ZADD,ZGND,SHNT(12),SNT
      REAL GADD(5),RP(12),Q(12),RPF(12),PF(12),V(12),LJ(22,22)
     +,LJIN(22,22),DELT(12),MPX(12),CST(12),QLIM(12)
      DO 6 I=1,12
           DO 6 J=1,12
                Y(I,J)=(0.00,0.00)
6     CONTINUE
      DO 9 I=1,12
           UKNT(I)=0
           UNT(I)=0
           NCODE(I)=0
           DELT(I)=0.0
           MPX(I)=0.0
           CST(I)=0.0
           RP(I)=0.0
           Q(I)=0.0
           QLIM(I)=0.0
9     CONTINUE
      IFT=1
      NUMB=0
      NPV=0
      LTOT=(0.00,0.00)
      READ(5,4)NODE,LIMIT,VSWING,JAC,IEG,IET,ICC
4     FORMAT(2I2,F6.4,4I1)
      V(1)=VSWING
      DELT(1)=0.00
      DO 100 I=1,NODE
           READ(5,105)J,ITC,VT,QM
105        FORMAT(I2,I1,F6.4,F7.3)
           IF(J.EQ.0)GO TO 101
           NCODE(J)=ITC
           IF(ITC.NE.1)GO TO 100
           NPV=NPV+1
           V(J)=VT
           QLIM(J)=QM
```

```
41 100   CONTINUE
42 101   KNUM=2*(NODE-1)-NPV
43       READ(5,7)PSTART,PINC
44 7     FORMAT(2F7.3)
45       DO 1 I=1,100
46            READ(5,2)B1,B2,ZL
47 2          FORMAT(2I2,2F8.6)
48            IF(B1.EQ.0)GO TO 5
49            Y(B1,B1)=Y(B1,B1)+1/ZL
50            Y(B2,B2)=Y(B2,B2)+1/ZL
51            Y(B1,B2)=Y(B1,B2)-1/ZL
52            Y(B2,B1)=Y(B2,B1)-1/ZL
53 1     CONTINUE
54 5     DO 11 I=1,NODE
55            READ(5,8)J,KUT,SNT
56 8          FORMAT(2I2,2F8.4)
57            IF(J.EQ.0)GO TO 20
58            UNT(J)=KUT
59            SHNT(J)=SNT
60 11    CONTINUE
61 20    DO 15 I=1,NODE
62            READ(5,10)J,TPF,PXT,CT,QSHT
63 10         FORMAT(I2,F5.3,F6.3,F7.3,F7.3)
64            IF(J.EQ.0)GO TO 3
65            PF(J)=TPF
66            FACT=1.0-(PF(J))**2
67            RPF(J)=SQRT(FACT)
68            MPX(J)=PXT
69            CST(J)=CT
70            Q(J)=QSHT
71            WRITE(6,12)J,PF(J),RPF(J)
72 12         FORMAT(1H0,4HNO. ,I2,4HPF= ,F5.3,5HRPF= ,F5.3)
73 15    CONTINUE
74 3     DO 14 J=2,NODE
75            RP(J)=CST(J)
76            IF((MPX(J).EQ.0).OR.(NCODE(J).EQ.1))GO TO 14
77            Q(J)=RP(J)*RPF(J)/PF(J)
78 14    CONTINUE
79       DO 28 I=1,NODE
80            READ(5,27)GBUS,ZGND
```

```
 81 27          FORMAT(I2,2F8.4)
 82             IF(GBUS.EQ.0)GO TO 30
 83             Y(GBUS,GBUS)=Y(GBUS,GBUS)+1/ZGND
 84 28      CONTINUE
 85 30      WRITE(6,29)
 86 29      FORMAT(1H1,13HPRIMARY Y-BUS)
 87         CALL POUTY(Y,NODE)
 88         FLAG=0
 89         WRITE(6,66)
 90 66      FORMAT(1H1,25HBASE SOLUTION FOR NETWORK)
 91 67      CALL NRLF(Y,RP,Q,NODE,V,NPV,KNUM,LJ,LJIN,DELT,NCODE,JAC
 92        +,QLIM,KK,IEG,IFT,IET,ICC)
 93         IF(KK.GE.20)GO TO 71
 94         NUMB=NUMB+1
 95         DO 21 I=2,NODE
 96              IF((V(I).GE.0.95).OR.(UKNT(I).GE.UNT(I)))GO TO 21
 97              Y(I,I)=Y(I,I)+1/SHNT(I)
 98              UKNT(I)=UKNT(I)+1
 99 21      CONTINUE
100         DO 68 J=2,NODE
101              RP(J)=RP(J)-MPX(J)*PINC
102              IF((MPX(J).EQ.0).OR.(NCODE(J).EQ.1).OR.
103        +     (NCODE(J).EQ.2))GO TO 68
104              Q(J)=RP(J)*RPF(J)/PF(J)
105 68      CONTINUE
106         IF(NUMB.LT.LIMIT)GO TO 67
107 71      STOP
108         END
109
110
111
112
113
114         SUBROUTINE SC(Y,Z,NODE)
115         REAL Z(22,22),Y(22,22)
116         DO 210 I=1,NODE
117              DO 210 J=1,NODE
118                   Z(I,J)=Y(I,J)
119 210     CONTINUE
120         DO 200 K=1,NODE
```

```
121             DO 240 I=1,NODE
122                  IF(I.EQ.K)GO TO 240
123                  DO 250 J=1,NODE
124                  IF(J.EQ.K)GO TO 250
125                  Z(I,J)=Z(I,J)-(Z(I,K)*Z(K,J))/Z(K,K)
126 250              CONTINUE
127 240         CONTINUE
128             Z(K,K)=-1/Z(K,K)
129             DO 275 M=1,NODE
130                  IF(M.EQ.K)GO TO 275
131                  Z(K,M)=Z(K,K)*Z(K,M)
132                  Z(M,K)=Z(K,K)*Z(M,K)
133 275         CONTINUE
134 200    CONTINUE
135        DO 280 I=1,NODE
136             DO 280 J=1,NODE
137                  Z(I,J)=-Z(I,J)
138 280    CONTINUE
139        RETURN
140        END
141
142
143
144
145
146        SUBROUTINE POUTY(P,NODE)
147        COMPLEX P(12,12)
148        DO 500 I=1,NODE
149             DO 500 J=1,NODE
150                  WRITE(6,520)I,J,P(I,J)
151 520              FORMAT(1HO,2HY(,I2,1H,,I2,3H)= ,E13.6,4H +J ,E13.6)
152 500    CONTINUE
153        RETURN
154        END
```

```
      SUBROUTINE NRLF(Y,RP,Q,NODE,V,NPV,KNUM,J,JIN,DELT,NCODE,JAC
     +,QLIM,KK,IEG,IFT,IET,ICC)
      REAL J(22,22),JIN(22,22),RP(12),Q(12),V(12),DELT(12)
     +,MM(22),TP(12),TQ(12),QLIM(12)
      COMPLEX Y(12,12),VC(12),SL(12,12),W(12),WK(12)
      INTEGER NCODE(12),GMT
      KNUM=2*(NODE-1)-NPV
      NRE=NODE-1
      GMT=2*NRE
      IF((IFT.EQ.0).AND.(ICC.EQ.1))GO TO 11
      DO 10 I=2,NODE
           IF(NCODE(I).EQ.1)GO TO 9
           V(I)=V(1)
 9         DELT(I)=0.00
 10   CONTINUE
      IFT=0
 11   DO 90 KK=1,20
 12   LVAR=0
      DO 20 L=1,NODE
           TP(L)=0.0
           TQ(L)=0.0
           DO 30 I=1,NODE
                REA=REAL(Y(I,L))
                AI=AIMAG(Y(I,L))
                PANGLE=DELT(L)-DELT(I)-ANGCHK(AI,REA)
                TP(L)=TP(L)+V(L)*V(I)*CABS(Y(I,L))*COS(PANGLE)
                TQ(L)=TQ(L)+V(L)*V(I)*CABS(Y(I,L))*SIN(PANGLE)
 30         CONTINUE
 20   CONTINUE
      LT=0
      JJ=NODE-1
      DO 25 L=1,JJ
           MM(L)=RP(L+1)-TP(L+1)
           IF(NCODE(L+1).EQ.1)GO TO 25
           LT=LT+1
           MM(LT+NODE-1)=Q(L+1)-TQ(L+1)
 25   CONTINUE
      FLAG=0
      DO 40 K=1,KNUM
           IF(ABS(MM(K)).GT.0.001)FLAG=1
 40   CONTINUE
```

```
      DO 39 L=1,NODE
           IF(NCODE(L).NE.1)GO TO 38
           IF(QLIM(L).EQ.0)GO TO 39
           IF(TQ(L).LT.QLIM(L))GO TO 39
           Q(L)=QLIM(L)
           NCODE(L)=2
           NPV=NPV-1
           KNUM=KNUM+1
           LVAR=1
           GO TO 39
38         IF(NCODE(L).NE.2)GO TO 39
           IF(V(L).LE.1.050)GO TO 39
           V(L)=1.050
           NCODE(L)=1
           NPV=NPV+1
           KNUM=KNUM-1
           LVAR=1
39    CONTINUE
      IF(LVAR.EQ.1)GO TO 12
      IF((FLAG.EQ.0).AND.(LVAR.EQ.0))GO TO 95
      IHD=NODE
      DO 45 N=1,NRE
           J(N,N)=0.0
           J(IHD,N)=0.0
           J(N,IHD)=0.0
           J(IHD,IHD)=0.0
           DO 50 M=1,NODE
                IF(M.EQ.N+1)GO TO 50
                REA=REAL(Y(N+1,M))
                AI=AIMAG(Y(N+1,M))
                PANGLE=DELT(N+1)-DELT(M)-
     +          ANGCHK(AI,REA)
                J(N,N)=J(N,N)-V(N+1)*V(M)*CABS(Y(N+1,M))
     +          *SIN(PANGLE)
                IF(NCODE(N+1).EQ.1)GO TO 50
                J(IHD,N)=J(IHD,N)+V(N+1)*V(M)* .
     +          CABS(Y(N+1,M))*COS(PANGLE)
                J(N,IHD)=J(N,IHD)+V(M)*CABS(Y(N+1,M))
     +          *COS(PANGLE)
```

```
240                   J(IHD,IHD)=J(IHD,IHD)+V(M)*
241        +          CABS(Y(N+1,M))*SIN(PANGLE)
242 50           CONTINUE
243              IF(NCODE(N+1).EQ.1)GO TO 45
244              REA=REAL(Y(N+1,N+1))
245              AI=AIMAG(Y(N+1,N+1))
246              PANGLE=-ANGCHK(AI,REA)
247              J(N,IHD)=J(N,IHD)+2*V(N+1)*CABS(Y(N+1,N+1))
248        +     *COS(PANGLE)
249              J(IHD,IHD)=J(IHD,IHD)+2*V(N+1)*
250        +     CABS(Y(N+1,N+1))*SIN(PANGLE)
251              IHD=IHD+1
252 45      CONTINUE
253             IHD=NODE
254             DO 55 N=1,NRE
255                  IHR=NODE
256                  IFG=0
257                  DO 60 M=1,NRE
258                       IF(M.EQ.N)GO TO 59
259                       REA=REAL(Y(N+1,M+1))
260                       AI=AIMAG(Y(N+1,M+1))
261                       PANGLE=DELT(N+1)-DELT(M+1)-ANGCHK(AI,REA)
262                       J(N,M)=V(N+1)*V(M+1)*CABS(Y(N+1,M+1))
263        +              *SIN(PANGLE)
264                       IF(NCODE(N+1).EQ.1)GO TO 46
265                       J(IHD,M)=-V(N+1)*V(M+1)*CABS(Y(N+1,M+1))
266        +              *COS(PANGLE)
267                       IFG=1
268 46                    IF(NCODE(M+1).EQ.1)GO TO 60
269                       J(N,IHR)=V(N+1)*CABS(Y(N+1,M+1))
270        +              *COS(PANGLE)
271                       IF(NCODE(N+1).EQ.1)GO TO 59
272                       J(IHD,IHR)=V(N+1)*CABS(Y(N+1,M+1))
273        +              *SIN(PANGLE)
274 59                    IHR=IHR+1
275 60                CONTINUE
276                  IF(IFG.EQ.1)IHD=IHD+1
277 55      CONTINUE
278             IF(JAC.EQ.1)GO TO 63
279             DO 61 I=1,KNUM
280                  DO 61 JJ=1,KNUM
```

```
280             DO 61 JJ=1,KNUM
281                  WRITE(6,62)I,JJ,J(I,JJ)
282 62               FORMAT(1HO,2HJ(,I2,1H,,I2,2H)=,E12.5)
283 61       CONTINUE
284
285 63       CALL SC(J,JIN,KNUM)
286
287          IS=2*(NODE-1)-NPV
288          DO 65 I=2,NODE
289               DT=0.0
290               DO 70 L=1,IS
291                    DT=DT+JIN(I-1,L)*MM(L)
292 70            CONTINUE
293               DELT(I)=DELT(I)+DT
294 65       CONTINUE
295          IBS=NODE-1
296          DO 110 I=NODE,GMT
297               VT=0.0
298               IF(NCODE(I-NODE+2).EQ.1)GO TO 110
299               IBS=IBS+1
300               DO 115 L=1,IS
301                    VT=VT+JIN(IBS,L)*MM(L)
302 115           CONTINUE
303               V(I-NODE+2)=V(I-NODE+2)+VT
304 110      CONTINUE
305          IF(IET.EQ.0)GO TO 90
306          WRITE(6,66)KK
307 66       FORMAT(1HO,6HAFTER ,I2,6H ITER.)
308          DO 67 I=1,NODE
309               WRITE(6,68)I,V(I),I,DELT(I)
310 68            FORMAT(1HO,2HV(,I2,2H)=,F11.5,3X,5HDELT(,I2,2H)=,F11.5)
311 67       CONTINUE
312
313 90       CONTINUE
314 95       WRITE(6,96)
315 96       FORMAT(1HO,60('*'))
316          WRITE(6,100)KK-1
317 100      FORMAT(1HO,25HLOAD FLOW SOLUTION AFTER ,I3,11H ITERATIONS)
318          WRITE(6,176)
319 176      FORMAT(1HO,26HINJECTED POWER AT EACH BUS)
320          DO 178 I=1,NODE
```

```
320         DO 178 I=1,NODE
321              WRITE(6,179)I,TP(I),TQ(I)
322  179        FORMAT(1H ,I2,5H: P= ,F8.4,4H Q= ,F8.4)
323  178    CONTINUE
324         DO 190 I=1,NODE
325              A=V(I)*COS(DELT(I))
326              B=V(I)*SIN(DELT(I))
327              VC(I)=CMPLX(A,B)
328  190    CONTINUE
329         DO 191 I=1,NODE
330              DO 191 JJ=1,NODE
331                   SL(I,JJ)=VC(I)*CONJG((VC(I)-VC(JJ))*(-Y(I,JJ)))
332  191    CONTINUE
333         WRITE(6,192)
334  192    FORMAT(1HO,10HLINE FLOWS)
335         DO 193 I=1,NODE
336              DO 193 JJ=1,NODE
337                   IF(SL(I,JJ).EQ.0)GO TO 193
338                   WRITE(6,194)I,JJ,SL(I,JJ)
339  194              FORMAT(1H ,I2,1H-,I2,4H P= ,F9.5,4H Q= ,F9.5)
340  193    CONTINUE
341         WRITE(6,175)
342  175    FORMAT(1HO,15HVOLTAGE PROFILE)
343         DO 180 I=1,NODE
344              WRITE(6,185)I,V(I),DELT(I)*180./3.1415
345  185         FORMAT(1H ,2HV(,I2,14H): MAGNITUDE= ,E13.6,
346        +      8H ANGLE= ,F11.6)
347  180    CONTINUE
348         IF(IEG.NE.1)GO TO 184
349         CALL EIGRF(J,KNUM,22,0,W,Z,0,WK,IER)
350         WRITE(6,181)
351  181    FORMAT(1HO,23HEIGENVALUES OF JACOBIAN)
352         DO 183 I=1,KNUM
353              WRITE(6,182)I,W(I)
354  182         FORMAT(1HO,2HW(,I2,2H)=,F10.5,3X,F10.5)
355  183    CONTINUE
356  184    RETURN
357         END
358
359
360
```

```
      FUNCTION ANGCHK(AI,REA)
      PI=4.0*ATAN(1.0)
      EPS=1.0E-10
      IF(ABS(REA).LT.EPS)GO TO 10
      ANGCHK=ATAN2(AI,REA)
      GO TO 20
10    IF(AI.LT.0.0)ANGCHK=-PI/2.0
      IF(AI.GT.0.0)ANGCHK=PI/2.0
      IF(ABS(AI).LT.EPS)ANGCHK=0.0
20    RETURN
      END
```